

**Imperial College London**  
**BCURA Agreement No: B82**  
**Improvements in Amine Flue Gas Scrubbing Systems for**  
**Coal Fired Power Plants**

Final Report

Project Duration: October 2006 - October 2009

University Project Manager:

Dr. C. S. Adjiman,  
Centre for Process Systems Engineering  
Department of Chemical Engineering  
Imperial College London, SW7 2AZ  
Tel: 020 7594 6638  
Fax: 020 7594 6606  
Email: c.adjiman@imperial.ac.uk

BCURA Industrial Supervisor:

Mr. N. Booth  
Power Technology Combustion and Emission Control Group  
Ratcliffe-on-Soar  
Nottinghamshire, NG11 0EE  
Tel: 0115 9362682  
Fax: 0115 9362205  
E-mail: nick.booth@eon-uk.com

# 1 Executive Summary

Mounting concern regarding the adverse effects associated with anthropogenically produced greenhouse gasses (GHG) has led governments to introduce binding legislation to limit and reduce the rate and magnitude of their emission of GHG, with particular emphasis on CO<sub>2</sub>. While there are many ways in which these ambitions could be achieved, so-called carbon capture and storage (CCS) is considered to be a promising route to attaining a meaningful reduction in CO<sub>2</sub> emissions in the near-term. It has been shown that CCS technology is particularly appropriate for large fixed-point emission sources. Of these, the fossil-fuel based power generation industry produces the lion's share of total global CO<sub>2</sub> emissions. Due to its technological maturity, operational flexibility and its associated low technology risk, post-combustion capture (PCC) of CO<sub>2</sub> via solvent based chemisorption is likely to be the preferred technology option in this important sector. However, current state-of-the-art PCC techniques have a significant energy penalty associated with their operation (OPEX) and due to the scale of the problem, the capital costs (CAPEX) associated with this technology are often considered prohibitive. Thus, there exists a well-recognised imperative for the significant reduction of both the size of the equipment required (CAPEX) and the cost of solvent regeneration (OPEX). The design of advanced solvents represents the best opportunity for reducing these costs as it is the solvent that defines the thermodynamic and kinetic limits of the process. However, conventional approaches to modelling reactive separation processes, due to their heavy reliance on the availability of extensive experimental data, do not easily lend themselves to reformulation as solvent design problems.

The goals of this project were the development and validation of detailed thermodynamic and process models relevant to CO<sub>2</sub> capture processes. The thermodynamic models have been developed using the SAFT-VR equation-of-state, and the process models have been implemented in the gPROMS modelling environment. We have developed a novel technique for modelling the phase behaviour and thermophysical properties of reactive fluid mixtures. Reliable models to quantify the phase and chemical equilibrium of mixtures of CO<sub>2</sub> + water + amine-based solvent have been developed. The solvent molecules considered include ammonia (NH<sub>3</sub>), methylamine, ethylamine, propylamine, butylamine, pentylamine, hexylamine, ethanol, monoethanolamine (MEA), 2-amino-2-methyl-1-propanol (AMP), diethylamine, diethanolamine (DEA), triethylamine, methyldiethylamine (MDEA). The models have been shown to be transferable so that the behaviour with other similar solvents (e.g. alkylamines or other alkanolamines) can be predicted in the absence of experimental data. The models obtained are highly accurate, with average absolute deviations less than 1.5% in saturated vapour pressure and liquid density.

Building on this success, we have proposed a new methodology for building accurate, predictive models of reactive separation processes, using rate-based models and taking advantage of the fact that CO<sub>2</sub> chemisorption is mass-transfer limited in commonly used solvents. The novel approach that has been developed has a significantly reduced dependence on experimental data when compared to other approaches. Further, due to the thermodynamic framework employed, the process models are substantially simpler and, in our experience, require no adjustment of model parameters as process operating conditions are changed or indeed as solvent blends are changed. We have validated the predictions of our absorber model using pilot plant data obtained from the International Test Centre in the University of Regina, Canada. This validation was performed with solvents with a wide range of reaction kinetics, thus giving confidence in our assumptions and results. The predictions of our desorber model have been validated using using pilot plant data obtained from NTNU in Trondheim, Norway. In this way, we have proposed a new approach for solving integrated solvent and process design problems in the context of mass-transfer limited reactive separation processes.

On the basis of preliminary results in this area, we now have the underpinning tools in place to design novel solvent blends, by optimising process performance (e.g., minimising energy consumption given separation targets). By building on other tools developed in the research group we can also tackle the issue of designing novel solvent molecules. Finally, to achieve a complete description of the design problem, we need to incorporate oxidation and corrosion models into our overall process model. All these offer promising and innovative avenues for further research.

Finally, from the work done in this project, results sufficient for eight journal papers have been obtained, of which one has been accepted for publication in *Industrial & Engineering Chemistry Research* with the remainder currently in preparation for journal publication and sixteen conference presentations, of which eleven were oral presentations, have been given.

# Contents

<b>1</b>	<b>Executive Summary</b>	<b>1</b>
<b>2</b>	<b>Introduction</b>	<b>5</b>
2.1	Background . . . . .	5
2.2	Chemistry and thermophysical property methods . . . . .	6
2.3	Approaches to modelling reactive separation systems . . . . .	8
2.3.1	Equilibrium vs. rate-based models . . . . .	8
2.3.2	Selection of a mass transfer model . . . . .	8
<b>3</b>	<b>Results and Discussion</b>	<b>9</b>
3.1	Thermodynamic modelling of reactive fluid mixtures with SAFT-VR . . . . .	9
3.1.1	Ammonia based mixtures . . . . .	12
3.1.2	Monoethanolamine based mixtures . . . . .	14
3.1.3	2-Amino-2-methyl-1-propanol based mixtures . . . . .	17
3.1.4	Overview of incorporation of chemical reactions within the SAFT approach	19
3.2	Process modelling and validation . . . . .	19
3.2.1	Model development and validation . . . . .	19
3.2.2	Initial solvent design study . . . . .	21
<b>4</b>	<b>Conclusions</b>	<b>22</b>
<b>5</b>	<b>Proposed work for a subsequent programme</b>	<b>23</b>

**6 Publications arising from the project**

**23**

Bibliography27

## 2 Introduction

### 2.1 Background

Due to their energy density, proven resource base and established infrastructure for their exploitation and distribution, it is well accepted that energy derived from fossil fuels will continue to play an important role in supplying the worlds energy [1]. At the same time, concerns surrounding climate change due to anthropogenic emissions of CO<sub>2</sub> have resulted in a number of initiatives to reduce CO<sub>2</sub> emissions [2]. So-called carbon capture and storage (CCS) technologies are accepted as being a promising route to a near-term meaningful reduction in CO<sub>2</sub> emissions. The power generation sector is the largest stationary point source of CO<sub>2</sub> emissions [3] and one of most viable technologies for CO<sub>2</sub> capture from power stations is post-combustion absorption of CO<sub>2</sub> with chemical solvents [4].

The current state-of-the-art technology is solvent scrubbing with amine based solvents [5]. However, this process is highly energy intensive, in particular it requires a significant amount of energy for solvent regeneration [6]. Therefore, there exists a strong imperative to reduce the energy penalty associated with CO<sub>2</sub> capture [7]. In order to achieve these goals, the selection and design of the solvent or solvent blend to be used is of utmost importance. Specifically, it is desirable that the energy penalty associated with solvent regeneration be decreased, the rate of reaction be increased and that the CO<sub>2</sub> loading capacity can be increased [7]. Therefore, this problem may be formulated as a solvent design problem, where proposed solvents and solvent blends can be evaluated using appropriate performance indices. Process performance indices help to quantify the overall solvent effect on the operation of the process. This leads to a tight integration of process operation and solvent selection, and provides a rational basis for solvent design [8].

Typically, in modelling systems with reactive separation, one either uses a sophisticated, computationally intensive methodology, such as in the work of Kucka *et al.* [9] or simplified enhancement factor concepts, such as in the work of van Swaaij *et al.* [10]. However, enhancement factors are exact only in a few special limiting cases, and typically approximations to describe more realistic scenarios are employed [11,12]. Moreover both approaches rely on experimental data to provide information on reaction kinetics and mass transfer. These data are unavailable in the context of novel solvents. Finally, in solvent design problems, there exists the paradoxical requirement to reduce as much as possible the computational complexity of the process model, while concurrently retaining accuracy in model predictions in order that the results of any optimisation

studies are as robust as possible [8].

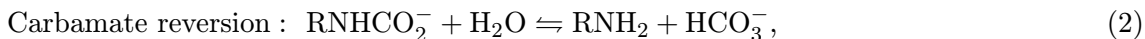
In this project, we have developed a new methodology for the design and assessment of novel solvent blends for fluid separation processes. Our approach is completely general and is equally applicable to both physical and chemical based separation processes with no change in model complexity, provided that the process is not kinetically limited. We use the statistical associating fluid theory for potentials of variable range (SAFT-VR) [13,14] both to account for the non-idealities that are observed in aqueous mixtures of amines and also to represent the key reactions that are present in this system, thereby simplifying the description of the chemical reactions at the level of the process model. Thus, the only experimental data required for assessing solvent blends are binary mixture vapour-liquid equilibria data, which are typically abundant, and are relatively easy to measure if they are not available, as opposed to detailed information on the kinetics and rate equations which are required in the usual approach. We propose that this approach provides a suitable platform for the solution of solvent design problems for complex and reacting fluid systems.

## 2.2 Chemistry and thermophysical property methods

The reactive nature of mixtures of amines in aqueous solution with  $\text{CO}_2$  is well known; there is a large body of experimental and theoretical work in place detailing the mechanisms and rates of these reactions [15–20]. Moreover, they have been presented several times in the literature, and as such they will not be described in detail here. It suffices to say that the principle reactions of interest are the formation of carbamate



and the subsequent reversion of carbamate to bicarbonate,



where it can be seen that the overall stoichiometry of the reaction is such that each molecule of  $\text{CO}_2$  is eventually associated with two amine molecules; the carbamate and protonated amine can be considered as a tightly bound ion pair (denoted by the square brackets) particularly at higher temperatures. In addition to these chemical reactions, there are also the ionic speciation

equilibria of the  $\text{CO}_2+\text{H}_2\text{O}$  and aqueous amine mixtures to consider [21]. The chemical reactions and ionic speciation that occur in these mixtures strongly influences the phase behaviour of the system, and failure to adequately account for these interactions results in highly erroneous predictions [22–24]. Typically, in order to account for the non-idealities of this mixture a quasichemical-based [25–28] lattice model of the liquid phase such as the electrolyte nonrandom two liquid (eNRTL) model of Chen *et al.* [29,30] (a modification of the NRTL model of Renon and Prausnitz [31]) is used, as in the work of Kucka *et al.* [9]. However, lattice models are inapplicable to the gas phase, and consequently, another theory must be used to describe its phase behaviour. Often, cubic equations-of-state, like the Soave-Redlich-Kwong [32] equation are used to describe the gas phase as in Kucka *et al.* [9], or sometimes the gas phase is treated as ideal as in the work of Kvamsdal *et al.* [33] or Ziaii *et al.* [34].

Others, such as Gabrielsen *et al.* [35] and Aboudheir *et al.* [36] have developed their own correlations using a Henry’s law type description of the phase behaviour, modified to incorporate the effect of the reactions on the vapour pressure of each component. Some of these models have been subsequently successfully incorporated in process models of  $\text{CO}_2$  absorption systems [37,38]. These correlations are typically very simple in mathematical form, and are very easy to use. However, their predictive ability is limited, and any attempt to use them outside the region in which the correlation was developed can result in highly unphysical predictions.

The development and implementation of accurate process models requires extensive calculation of the physical properties associated with the system. Thus, the ability to calculate and, more importantly, accurately and reliably predict the phase behaviour and thermophysical properties of complex, multicomponent systems is of paramount importance to developing robust process models. In this way, accurate physical property predictions can be considered the raw materials of optimal process design [39]. The implementation of a multistage nonequilibrium model involves the repeated calculation of interfacial compositions (phase equilibria) and the enthalpies of the bulk gas and liquid phases requiring the calculation of both pure component and mixture enthalpies. As these quantities are themselves used again and again throughout the model in the energy balance and rate equations, their accurate calculation is of vital importance to the accuracy of the the model as a whole. Further, many of the correlations used in typical engineering design require the calculation of quantities such as liquid interfacial tension, enthalpy of vapourisation, heat capacity, gas and liquid densities. The ability to accurately calculate these quantities in a predictive way with SAFT-VR will remove existing restrictions on exploring with confidence the different operating regimes and also allow more confidence in solvent design activities. We have used the SAFT-VR [13,14,40,41] equation of state (EOS) to calculate the thermodynamic



properties and fluid phase equilibria of our system as it has previously been shown to model complex associating and reactive mixtures successfully for a wide range of conditions.

## **2.3 Approaches to modelling reactive separation systems**

### **2.3.1 Equilibrium vs. rate-based models**

Most types of gas-liquid contactors can be considered as a cascade of segments or stages which are related to one another through mass and energy balance equations [42]. In figure 14, different model approaches representing different complexities concerning the description of mass transfer and chemical reaction are presented. The simplest model is the classical equilibrium stage model which assumes that the streams leaving a given stage are in equilibrium, with no reactions and infinitely fast mass transport within the single stage [42]. As mass and heat transfer are rate processes that are driven by gradients of chemical potential and temperature, equilibrium is rarely attained and thus traditional “equilibrium stage models + efficiency factor” approaches are inadequate for the description of chemisorption processes. In increasing the complexity of the model, we can choose to include some details of the reaction kinetics while maintaining the concept of the equilibrium stage [43].

For a model to be both rigorous and predictive, the effect of simultaneous heat and mass transfer, the effect of chemical reactions and their coupled effects on the physical properties and phase behaviour of the system must be included in the model. Mass transfer in multicomponent mixtures is more complicated than in binary systems because of the possible coupling between the individual concentration gradients. Phenomena such as reverse diffusion (diffusion of a species against its own concentration gradient) or osmotic diffusion (diffusion of a species even though no concentration gradient for that species exists) are possible in multicomponent systems but not in binary mixtures. One of the interesting consequences of these interaction effects is that the individual point efficiencies of different species are not constrained to lie between zero and one. Instead, they may be found anywhere in the range from  $-\infty$  to  $+\infty$  [44]. It is not possible to predict these phenomena with “equilibrium stage” models.

### **2.3.2 Selection of a mass transfer model**

For reactive systems with a “fast” chemical reaction, i.e., where the process is not limited by the reaction kinetics, the two-film model has been extensively used as the mass transfer model

of choice almost since its inception by Lewis and Whitman in 1924 [45] and its subsequent refinement by Hatta in 1932 [46]. See for example the journal papers of [33, 42, 44, 47–50] and references therein for details. Also, it has been shown [51] that the selection of the film model can be justified on the basis of the value of  $Ha$ , the Hatta number [52, 53]. It has been shown that systems characterised by a “rapid” chemical reaction, such as the absorption of acid gases, where the chemical reaction can be considered to occur only in the liquid film, the liquid holdup is not important and the rate of absorption will be large if the effective interfacial area and the individual mass transfer coefficients are large. This is called the physical kinetic regime and is characterised by the condition:

$$Ha > 3 \tag{3}$$

The Hatta,  $Ha$ , number may be defined as [54]:

$$Ha = \frac{N_i}{N_i^{Phys}} \tag{4}$$

This is the ratio of absorption with reaction,  $N_i$ , to that without reaction,  $N_i^{Phys}$ .  $Ha$  has different functional forms depending on the nature of the reaction occurring (1<sup>st</sup> order 2<sup>nd</sup> etc). As long as the condition in equation (3) is satisfied, the system will be well represented by the two-film model.

### 3 Results and Discussion

This section is presented in three successive parts. First, some key results of the thermodynamic modelling activities of this project are presented. This section is divided into three distinct sections wherein the results of the work on NH<sub>3</sub>, MEA and AMP mixtures are presented. Subsequently, the results of our process model development and validation work are presented. Finally we present the results of our initial solvent design work.

#### 3.1 Thermodynamic modelling of reactive fluid mixtures with SAFT-VR

In the SAFT-VR approach a molecule  $i$  is modelled as a homonuclear chain of  $m_{ii}$  bonded square-well segments of hard-core diameter  $\sigma_{ii}$ . The square-well interactions are further characterised

by a well depth  $\varepsilon_{ii}$  and a range  $\lambda_{ii}$ . In addition, a number of off-centre, square-well association sites are used to mediate the association interactions. The sites are placed at a distance  $r_d^* = 0.25$  from the centre of a segment and the cut-off range between a site  $a$  on a segment  $i$  and a site  $b$  on a segment  $j$  is denoted by  $r_{c,ab,ij}^* = r_{c,ab,ij}/\sigma_{ij}$ . These two parameters define the volume  $K_{ab,ij}$  available for site-site bonding [55]. When two sites are within a distance of  $r_{c,ab,ij}$  they interact with a well depth  $\varepsilon_{ab,ij}^{HB}$ . The sites are commonly labelled as  $e$  or  $H$ , representing either an electronegative atom (or its lone-pairs of electrons) or the hydrogen atoms in a molecule, respectively; only  $e$ - $H$  bonding is allowed. In all the models considered in this paper one  $e$  site is allocated for each electron lone-pair and one  $H$  site for each hydrogen atom.

In order to model the mixtures, a number of unlike intermolecular potential parameters also need to be specified. The arithmetic mean is used to obtain size-related intermolecular parameters, so that the unlike contact diameter between two molecules  $i$  and  $j$  is given by

$$\sigma_{ij} = \frac{\sigma_{ii} + \sigma_{jj}}{2}, \quad (5)$$

the unlike square-well range by

$$\lambda_{ij} = \frac{\lambda_{ii}\sigma_{ii} + \lambda_{jj}\sigma_{jj}}{\sigma_{ii} + \sigma_{jj}}, \quad (6)$$

and the unlike bonding volume by

$$K_{ab,ij} = \left[ \frac{K_{ab,ii}^{1/3} + K_{ab,jj}^{1/3}}{2} \right]^3. \quad (7)$$

These parameters are not readjusted at any point. The unlike dispersion and hydrogen bonding energetic parameters are defined in terms of the geometric mean of the like interactions and a correction factor, so that the unlike dispersion energy between two components  $i$  and  $j$  is given by

$$\varepsilon_{ij} = (1 - k_{ij})\sqrt{\varepsilon_{ii}\varepsilon_{jj}}, \quad (8)$$

and the unlike hydrogen bonding energy between two sites  $a$  and  $b$  is given by

$$\varepsilon_{ab,ij}^{HB} = (1 - k_{ab,ij}^{HB})\sqrt{\varepsilon_{ab,ii}^{HB}\varepsilon_{ab,jj}^{HB}}. \quad (9)$$

The adjustable parameters  $k_{ij}$  and  $k_{ab,ij}^{HB}$  are determined by comparison to mixture experimental data.

In reporting the performance of our models, we use the average absolute deviations AAD. For the pure components, we use three descriptors of the quality of the fit: an overall percentage AAD,

$$\%AAD = \frac{100}{N_P + N_\rho} \left\{ \sum_{i=1}^{N_P} \left| \frac{P_{v,i}^{\text{Exp}}(T_i) - P_{v,i}^{\text{Calc}}(T_i; \theta)}{P_{v,i}^{\text{Exp}}(T_i)} \right| + \sum_{j=1}^{N_\rho} \left| \frac{\rho_{l,j}^{\text{Exp}}(T_j) - \rho_{l,j}^{\text{Calc}}(T_j; \theta)}{\rho_{l,j}^{\text{Exp}}(T_j)} \right| \right\}, \quad (10)$$

and separate percentage AADs for vapour pressure and liquid density,

$$\%AAD P = \frac{100}{N_P} \sum_{i=1}^{N_P} \left| \frac{P_{v,i}^{\text{Exp}}(T_i) - P_{v,i}^{\text{Calc}}(T_i; \theta)}{P_{v,i}^{\text{Exp}}(T_i)} \right|, \quad (11)$$

$$\%AAD \rho_l = \frac{100}{N_\rho} \sum_{i=1}^{N_\rho} \left| \frac{\rho_{v,i}^{\text{Exp}}(T_i) - \rho_{v,i}^{\text{Calc}}(T_i; \theta)}{\rho_{v,i}^{\text{Exp}}(T_i)} \right|. \quad (12)$$

In the case of the mixtures, we report either the error in the calculated equilibrium pressure of the mixture, at a given temperature and liquid composition given by

$$\%AAD P = \frac{100}{N_P} \sum_{i=1}^{N_P} \left| \frac{P_i^{\text{Exp}}(T, x_i^{\text{I}}) - P_i^{\text{Calc}}(T, \rho^{\text{I}}, x_i^{\text{I}}; \theta, \phi)}{P_i^{\text{Exp}}(T, x_i^{\text{I}})} \right|, \quad (13)$$

or the error in the calculated equilibrium temperature at given pressures and liquid compositions

$$\%AAD T = \frac{100}{N_T} \sum_{i=1}^{N_T} \left| \frac{T_i^{\text{Exp}}(P_i, x_i^{\text{I}}) - T_i^{\text{Calc}}(P_i, \rho^{\text{I}}, x_i^{\text{I}}; \theta, \phi)}{T_i^{\text{Exp}}(P_i, x_i^{\text{I}})} \right|, \quad (14)$$

and, if available, the error in the composition of the other equilibrium (vapour or liquid) phase at each  $T_i$  or  $P_i$  and phase I composition. As mole fractions are constrained to be between zero and one, an absolute measure of error is more appropriate,

$$AAD x^{\text{II}} = \frac{1}{N_x} \sum_{i=1}^{N_x} \left| x_i^{\text{II,Exp}} - x_i^{\text{II,Calc}} \right|. \quad (15)$$

### 3.1.1 Ammonia based mixtures

#### Pure ammonia

Following the general scheme described in section 3.1,  $\text{NH}_3$  is modelled as a single spherical segment. This is what one would expect as a model  $\text{NH}_3$  and the spatial density plots presented by Thompson *et al.* [56] lend further credence to this view. The hydrogen bonding interactions in  $\text{NH}_3$  are mediated by the inclusion of four off-centre association sites. A four-site model is physically intuitive, and is consistent with the traditional physical chemistry molecular-orbital view of ammonia and it is also consistent with the view of water for which there is abundant simulation and experimental data, as presented by Clark *et al.* [57]. The four-site model is asymmetric, with one  $e$  site to represent the lone pair of electrons on the nitrogen atom and three  $H$  sites to represent the three hydrogen atoms. When modelling  $\text{NH}_3$ , only  $e - H$  interactions are permitted. A final model of  $\text{NH}_3$  is selected based on its ability to simultaneously correlate vapour-liquid equilibria and predict the interfacial-tension,  $\gamma$ , and the enthalpy of vapourisation,  $\Delta H_{fg}$  of the  $\text{NH}_3$  molecule. As  $\Delta H_{fg}$  is a second derivative property of the Helmholtz free energy, this constitutes a very severe test of our model. Further, this analysis of  $\gamma$  is helpful in establishing that we have the correct partitioning between the enthalpic and entropic contributions to the free energy, as from

$$dA^\sigma = -SdT^\sigma - PdV^\sigma + \gamma d\mathcal{A} + \sum_i^{nc} \mu_i dn_i \quad (16)$$

it can be seen that

$$\left(\frac{dA^\sigma}{dT}\right)_{V^\sigma, \mathcal{A}, n_i} = -S^\sigma$$

The results of this investigation are shown in figures 1, 2, 3a and 3b respectively. The AAD as defined by equation (10) for the  $\text{NH}_3$  model was 1.48% in saturated vapour pressure and liquid density. We consistently use this rationale to discriminate between molecular models for other components considered in this work.

#### Aqueous ammonia mixtures

The modelling of binary mixtures of  $\text{NH}_3 + \text{H}_2\text{O}$  is interesting both from a practical and scientific standpoint. The academic interest stems primarily from the fact that aqueous solutions of  $\text{NH}_3$

significantly disassociate in water. In this work, we treat this dissociation without explicitly treating the electrolytes, thus simplifying the model. In solutions with significant dissociation, there will be significant deviation from Henry's law. This is significant as a failure to adequately account for these interactions between  $\text{NH}_3$  and  $\text{H}_2\text{O}$  will result in an erroneous prediction of vapour pressures [24]. From a more practical perspective, there has been a great deal of recent interest in using  $\text{NH}_3$  as an alternative solvent with which to capture  $\text{CO}_2$ . Obviously, before  $\text{NH}_3$  can be deployed in practice, a detailed knowledge of the phase behaviour of aqueous  $\text{NH}_3$  mixtures and also the liquid phase behaviour of aqueous  $\text{NH}_3 + \text{CO}_2$  mixtures is essential.

The  $\text{NH}_3 + \text{H}_2$  mixture is a mixture of two associating fluids of similar molecular weight, it is completely miscible and does not exhibit azeotropy. One would therefore expect the unlike interactions in the system to be close to ideal. Consequently, the standard Lorentz-Berthelot (LB) [58] combining rules should be an appropriate choice in this case. Unlike binary interaction parameters were estimated by comparison with experimental data from the triple-point,  $T_t$  of  $\text{H}_2\text{O}$  to the critical point,  $T_c$  of  $\text{NH}_3$ . This estimation was performed using the gPROMS software package [59]. A sample of graphical results are provided in figure 4. The accuracy of this model as defined by equation (13) and (14) is 1.857% in temperature and pressure and 0.026 in mole fraction as defined by equation (15). This mixture exhibits both positive and negative deviations from Raoult's law as well as extensive ionic speciation, and it is gratifying to see this feature reproduced with our model.

### **Ammonia ternary mixtures**

The immediate industrial relevance of this work is in the arena of amine based  $\text{CO}_2$  capture from the flue gases of fossil fuel fired power plants, so one obvious application of these results is in the modelling, simulation and optimisation of such processes. Recently, there has been a significant amount of industrial interest in  $\text{NH}_3$  based  $\text{CO}_2$  capture processes [60–63], and accurate thermophysical models of this system are necessary for the development of accurate and predictive process models. However, the complexity associated with modelling this mixture is compounded by the fact that it is reactive, as opposed to simply associating. In modelling the  $\text{NH}_3 + \text{H}_2\text{O} + \text{CO}_2$  mixture, SAFT-VR intermolecular parameters describing the  $\text{NH}_3 + \text{CO}_2$  interactions were obtained using the experimental data presented by Goppert *et al.* [64].

Maurer [22] notes that if one is using a chemical-theory to calculate the phase equilibrium of the reacting  $\text{NH}_3 + \text{H}_2\text{O} + \text{CO}_2$  mixture, there are - in principle - 72 temperature dependent binary interaction parameters which must be determined. It is unrealistic to assume that these parameters can be determined by comparison with experimental VLE data, and as a result

sensitivity analyses must be performed, and parameters of minor importance either estimated or ignored. This further level of approximation in the approach inevitably reduces the accuracy and predictivity of the models. In the SAFT approach, only five temperature-independent binary-interaction parameters are required, and reliable values for these parameters can be obtained by fitting to binary mixture VLE data. Of these, only two need be determined by comparison to ternary VLE data. A sample of calculation results at conditions relevant to CCS processes are presented in figures 5 and 6. We note that the unlike interaction parameters for the  $\text{NH}_3+\text{CO}_2+\text{H}_2\text{O}$  mixture were fitted to the data shown in figure 5, while the results presented in figure 6 are predictions. Our simple, physical models predict the phase behaviour of this complex mixture very accurately - the models developed for this mixture correlate and predict the liquid phase  $\text{CO}_2$  loading to within 0.02.

### 3.1.2 Monoethanolamine based mixtures

In this section, a brief description of the development of a detailed SAFT-VR model of monoethanolamine (MEA) is presented. In a recent publication [65], we describe in detail the development of the SAFT-VR models of  $\text{H}_2\text{O}$ , MEA and  $\text{CO}_2$ , and readers are referred here and to references therein for a complete description of the methods employed in the development of SAFT-VR molecular models.

#### Pure monoethanolamine

Here we present a model of MEA that explicitly considers that the hydroxyl – hydroxyl interaction, the amine – amine interaction, the hydroxyl electron lone-pair – amine hydrogen and the hydroxyl hydrogen – amine electron lone-pair interactions all have different hydrogen bond energies. Inevitably, this increases the number of intermolecular parameters required to model the multifunctional nature of MEA, but one can exploit the molecular nature of the SAFT theory to reduce the number of intermolecular parameters that have to be determined by transferring parameters from other molecules with the same functional groups: SAFT-VR models of ethanol and ethylamine. In this way, we present a general methodology for the development of accurate, predictive models of complex, multifunctional, associating molecules, and their mixtures with other associating fluids.

The model of MEA is characterised by twelve parameters:  $m_{MEA}$ ,  $\sigma_{MEA}$ ,  $\varepsilon_{MEA}$ ,  $\lambda_{MEA}$ ,  $\varepsilon_{eH,MEA}^{\text{HB}}$ ,  $r_{c;eH,MEA}$ ,  $\varepsilon_{e^*H^*,MEA}^{\text{HB}}$ ,  $r_{c;e^*H^*,MEA}$ ,  $\varepsilon_{eH^*,MEA}^{\text{HB}}$ ,  $r_{c;eH^*,MEA}$ ,  $\varepsilon_{e^*H,MEA}^{\text{HB}}$  and  $r_{c;e^*H,MEA}$ , which results in a parameter estimation problem of much higher dimensionality than is usual

in SAFT-VR studies of associating systems. At this point, we take advantage of the physical basis and transferability of parameters in SAFT (see for example the studies reported in references [66, 67]) and propose to transfer the association parameters describing the interaction between the hydroxyl groups of the MEA molecules (represented by the  $e - H$  site-site interaction:  $\varepsilon_{eH,MEA}^{HB}$ ,  $r_{c;eH,MEA}$ ) from those obtained in a separate study for ethanol. Similarly, the parameters related to the interaction between the amine groups of MEA (represented by the  $e^* - H^*$  site-site interaction:  $\varepsilon_{e^*H^*,MEA}^{HB}$ ,  $r_{c;e^*H^*,MEA}$ ) are determined from a separate study for ethylamine. When these parameters for ethanol and ethylamine are transferred for the corresponding interactions in MEA, the only association interactions that remain to be specified for the MEA molecule are those for the cross amine-hydroxyl group association interactions. These are represented by  $e^* - H$  and  $e - H^*$  site-site interactions characterised by  $\varepsilon_{e^*H,MEA}^{HB}$ ,  $r_{c;e^*H,MEA}$ ,  $\varepsilon_{eH^*,MEA}^{HB}$  and  $r_{c;eH^*,MEA}$ . To reduce further the number of parameters, we set the value of the range of the association potential for the  $e - H^*$  and  $e^* - H$  interactions to be the same such that  $r_{c;eH^*,MEA} = r_{c;e^*H,MEA}$ . The %AAD (equation (10)) is not improved by using two different values for  $r_{c;eH^*,MEA}$  and  $r_{c;e^*H,MEA}$ . The proposed procedure has allowed us to reduce the number of parameters to six ( $\sigma_{MEA}$ ,  $\varepsilon_{MEA}$ ,  $\lambda_{MEA}$ ,  $\varepsilon_{eH^*,MEA}^{HB}$ ,  $\varepsilon_{e^*H,MEA}^{HB}$  and  $r_{c;eH^*,MEA}$ ), no more than for other SAFT-VR models.

The performance of the final model of MEA can be seen in figures 1 and 2. The predictions obtained for the enthalpy and the surface tension (figures 8 and 9) in particular are in excellent agreement with the experimental data [68–71]. It is striking to see how the set of selected molecular parameters is able to quantitatively predict the surface tension values over a wide range of temperatures and pressures. The AAD as defined by equation (10) for the MEA model was 2.41% in saturated vapour pressure and liquid density. These results give added confidence in the adequacy of the model developed for the complex MEA molecule.

### Aqueous MEA mixtures

A mixture of MEA and  $H_2O$  modelled using the asymmetric model of MEA presented above requires the determination of three adjustable unlike energy interaction parameters: the hydrogen bonding energy between water and the hydroxyl ( $\varepsilon_{eH,MEA-H_2O}^{HB} = \varepsilon_{He,MEA-H_2O}^{HB}$ ) and amine ( $\varepsilon_{e^*H,MEA-H_2O}^{HB} = \varepsilon_{H^*e,MEA-H_2O}^{HB}$ ) groups of MEA, and the unlike dispersion interactions between MEA and water  $\varepsilon_{MEA-H_2O}$ . In order to reduce the number of mixture parameters, a transferable approach is proposed. The hydrogen-bonding interaction between the hydroxyl group of MEA and water is transferred from that of a mixture of ethanol and water and, similarly, the hydrogen-bonding interaction between the amine group and water is transferred from



a study of ethylamine and water.

In figure 10, three isotherms of the vapour-liquid equilibrium for MEA+H<sub>2</sub>O at  $T= 298.15, 343.15, 364.15$  K are presented; the adequacy of the description can be clearly seen from the figure. The continuous lines represent calculations performed with the asymmetric model of MEA and the dashed lines represent calculations performed with the symmetric model. The accuracy of the models in describing the MEA+H<sub>2</sub>O mixture is %AAD=2.03% in temperature and pressure and AAD=0.024 in vapour phase composition when using the asymmetric model of MEA and %AAD=4.39% in temperature and pressure and AAD=0.008 in vapour phase composition when using the symmetric model of MEA.

### MEA ternary mixtures

Armed with the molecular models for pure component and binary mixtures developed in the previous sections, we now come to a main goal of our work: the accurate representation of the fluid phase behaviour of carbon dioxide in aqueous MEA. Numerous studies of the thermophysical properties of the MEA+CO<sub>2</sub>+H<sub>2</sub>O mixture have been reported to date. There are also a substantial number of correlations which describe the vapour-liquid equilibria of this system. The majority of these expressions are however applicable only over a limited range of compositions and/or temperature and pressure. Outside the recommended range, these expressions are typically inapplicable and are therefore of limited use in the design and optimisation of novel processes incorporating these components. One major advantage of the SAFT approach is that the parameters used in the models are temperature and pressure independent and thus there is in principle no region in the fluid range beyond description (with due caution taken in the critical and near-critical regions). A caveat, however, in the context of the MEA+CO<sub>2</sub>+H<sub>2</sub>O system, is that our models do not fully capture the various reaction mechanisms (we focus on the formation of carbamate), so that use of the model far outside the region where the models are developed may not be reliable (e.g., in the limit of low water concentration).

In modelling MEA + CO<sub>2</sub> + H<sub>2</sub>O, we examine data over a temperature range from 298.15K to 373.15K, a pressure range from 0.001MPa to 10MPa, and a liquid phase CO<sub>2</sub> concentration of  $0.01 \leq x_{CO_2} \leq 0.12$  [72–74]. We have used the data at 313 K to estimate the MEA–CO<sub>2</sub> association energy  $\varepsilon_{e^*\alpha, MEA-CO_2}^{HB}$  using the gPROMS software package [59] assuming that  $\varepsilon_{MEA-CO_2}$  is given by the Berthelot rule, i.e.,  $k_{MEA-CO_2} = 0.0$ . Using these parameters we are able to obtain an excellent description of the ternary system at these conditions and excellent quantitative predictions of the ternary phase behaviour at 333 K and 335 K, with an AAD over the three isotherms of 0.010 in liquid mole fraction of CO<sub>2</sub>, for MEA represented as the asymmetric

model. This level of accuracy is in line with that presented in other contributions, for example the recent work of Faramazi *et al.* [21]. We note that, unlike the many correlations that are currently available, our model captures the behaviour of the data over the entire composition range for which data is available.

The results of our SAFT-VR calculations for the phase equilibrium of MEA+CO<sub>2</sub>+H<sub>2</sub>O are summarised in figure 11. As can be seen, a complex, non-linear behaviour is seen for the partial pressure of CO<sub>2</sub> of the coexisting gas phase as a function of the liquid phase CO<sub>2</sub> mole fraction (the latter is a direct measure of the extent of absorption of CO<sub>2</sub> in the amine solvent). This behaviour is due to a complex system of competing interactions, and it is very encouraging to see this behaviour reproduced so accurately with our simple physical models of the chemical association. From figure 11, one can also see that, though the various correlations can be used to provide a good description of the absorption, their use is not appropriate over wide ranges of conditions. Further, in figure 11a we compare the results of using both the symmetric and asymmetric models of MEA to predict the phase behaviour of this mixture. It can be seen that while the asymmetric model fully captures the complex fluid phase behaviour, the symmetric model does not. This is because a fully symmetric model of MEA misrepresents the stoichiometry of the corresponding reactions of this system, and results in a vapour phase consisting almost entirely of water. Finally, we have found that the inclusion of nitrogen (an essentially inert gas, chemically speaking) in our SAFT-VR description does not modify the phase behaviour of the liquid phase appreciably. This accurate representation of the fluid phase behaviour of MEA + CO<sub>2</sub> + H<sub>2</sub>O (+N<sub>2</sub>) within our SAFT-VR platform is of paramount importance for use in a detailed description of the CO<sub>2</sub> capture process. Again, our models predict the phase behaviour of this complex mixture very accurately - the models developed for this mixture correlate and predict the liquid phase CO<sub>2</sub> mole fraction with an accuracy of 0.0165 of CO<sub>2</sub> mole fraction in the liquid phase.

### 3.1.3 2-Amino-2-methyl-1-propanol based mixtures

Following the results of our study of MEA, we proceed to build models of 2-amino-2-methyl-1-propanol (AMP). Apart from MEA, AMP is one of the most studied alkanolamine alternatives for CO<sub>2</sub> capture. This is because it is the sterically hindered form of MEA, and therefore differences between the properties of AMP and MEA can unambiguously be ascribed to steric effects. Given the results of the MEA work, we have a clear direction as to how to model AMP.

## Pure AMP

A detailed model of AMP has been developed, preserving the molecular detail of the molecule by once again considering an asymmetric model of this compound. In order to reduce model complexity, all association parameters required to describe AMP are transferred from the MEA model. This is a reasonable decision, as both molecules are primary alkanolamines, and this is consistent to group contribution approaches. Thus, AMP is modelled as having an aspect ratio of 2.29, with the same association scheme as MEA. Again, results of the models developed for AMP are presented in figures 1 and 2. The AAD as defined by equation (10) for the AMP model was 0.29% in saturated vapour pressure and liquid density.

## Aqueous AMP mixtures

Again, following the MEA mixture modelling, we transfer binary interaction parameters describing the unlike interactions between AMP and H<sub>2</sub>O from the work on MEA. In this case, an excellent description of the binary vapour-liquid equilibria is obtained without adjusting any binary interaction parameters. The accuracy of this model as defined by equation (13) and (14) is 0.42% in temperature and pressure and 0.006 in mole fraction as defined by equation (15). The transferable nature of the parameters developed to describe these complex mixtures is a testament to the adequacy of our models and the rigorous physical basis of the SAFT approach. Results of this work are provided in figure 12.

## AMP ternary mixtures

Once again, it is necessary to develop models of AMP+CO<sub>2</sub>+H<sub>2</sub>O. We do this in a similar manner to the MEA work. Results are presented in figure 13. We note that this is a prediction, with the unlike interaction parameters describing the AMP+CO<sub>2</sub> interactions having been obtained from a separate data set at  $T = 313.15\text{K}$ . This is a highly complex system, with numerous competing interactions, and a high accuracy is achieved with relatively simple physical interpretations of these interactions that nevertheless account for the complex, non-linear behaviour of this system. Again, our models predict the phase behaviour of this complex mixture very accurately - the models developed for this mixture correlate and predict the liquid phase CO<sub>2</sub> mole fraction with an accuracy of 0.02 of CO<sub>2</sub> mole fraction in the liquid phase.

### 3.1.4 Overview of incorporation of chemical reactions within the SAFT approach

We incorporate a description of the many interactions between the fluid components at the level of the thermodynamic model, using the SAFT formalism to simultaneously mediate the effect of the physical and chemical interactions in the fluid. This approach facilitates a consistent, physically based description of the numerous, competing interactions in both the gas and liquid phases, giving full consideration to all aspects of the non-ideality of this mixture. Moreover, the SAFT approach allows implicit consideration of reaction products, i.e., when compounds  $A$  and  $B$  react to form a product  $C$ , the product is described in the SAFT-VR model as an  $A$ - $B$  dimer, possessed of thermophysical properties which are defined by the unlike interaction parameters of components  $A$  and  $B$ . This both simplifies the mass and energy balance equations in the process model (i.e., there are no generation terms in these balance equations), and also removes the requirement for an explicit description of the properties of the reaction products. Finally, because reactions are incorporated in the physical description of the fluid, we no longer need to use enhancement factor concepts to describe the effects of chemical reaction on the process behaviour. We are therefore no longer constrained by the availability of experimental data on the rate equations in reacting systems. This constitutes a major advantage in modelling systems comprising novel solvents where these experimental data are not available. A caveat to this approach is that it may not be appropriate in systems which are not limited by the kinetics of the chemical reaction occurring.

## 3.2 Process modelling and validation

### 3.2.1 Model development and validation

The model described in this section has been implemented using the commercial software package gPROMS [59] using a SAFT-VR Foreign Object [75].

Reactive separation processes are highly studied, but some significant challenges remain in developing predictive models of these processes. Principally, conventional models developed for these processes require a large amount of experimental data to describe the effects of both the physical interactions and chemical reactions on process behaviour. Further, so-called enhancement factors are typically used to describe the accelerating effect of the reactions on the mass transfer. However, these expressions are theoretically exact only in a few limiting cases, and typically simplifications or approximations are used in practice. Moreover, enhancement factor

expressions themselves require a lot of experimental information pertaining to the rate equations and reaction kinetics associated with the system at hand. All this conspires to make predictive modelling and solvent design difficult.

The SAFT-based approach which we have employed in our work significantly simplifies the modelling of mass-transfer limited reactive separation systems. In our model, reaction products are implicitly considered in the thermodynamic model of the fluid, as opposed to explicitly at the level of the process model. This means less physicochemical properties are required to describe the process behaviour. Moreover, there are fewer component balances required, and there are no generation terms in the mass or energy balance equations. Finally, because of this, there is no enhancement factor required to describe the effect of the reaction.

In order for us to have confidence in the predictions of our model, we must ensure that it predicts accurately temperature and composition profiles along the length of the column, rather than simply the conditions at the outlet of the column [76]. Therefore, we validate the predictions of both our absorber and desorber models using published pilot plant data. To test the robustness of the assumption of reaction equilibrium, we assess the adequacy of our model against both MEA and AMP solvents, i.e., solvents which are considered to have both ‘fast’ and ‘slow’ kinetics. Finally, we note that no adjustable parameters are used in the process model. The results presented in this section are predictions.

For the absorber model presented in this paper, the required input to the model, in addition to the column geometry and packing characteristics, the inlet gas phase pressure, temperature, flowrate and composition and the inlet liquid temperature, flowrate and composition. The validation of the proposed absorber model is performed by comparison of the model predictions with experimental data presented by Tontiwachwuthikul *et al.* [49] for the data presented for runs T22 and T26. The results presented in figure 17 were obtained using an MEA solvent and those results presented in figure 17 were obtained using an AMP based solvent solution. The results of these investigations are shown in figures 16 - 17. These data were chosen as they have previously been independently reproduced by other workers [9,37]. Good agreement is observed between the measured and simulated column profiles, particularly in light of the simplicity of the proposed model. The accuracy of the predictions of our absorber model are in line with other contributions in the literature. We emphasise the fact that no enhancement factors were used in this work, nor were any kinetic data (rate constants, reaction enthalpies etc) required. Moreover, no retuning of model parameters or correlations was required in switching between MEA and AMP solvents. On this basis, we consider that we have provided rigorous validation

of our assumptions, and that our model is robust. Consequently, we propose that this model is a suitable initial point for the construction of a platform for the solution of solvent design problems in reactive separation systems.

In the case of the desorber model, in addition to the column geometry and packing characteristics, the required inputs are the inlet liquid flowrate, temperature, pressure and composition. The inlet steam flowrate and pressure are assigned in the model, and may be used to either provide a given amount of energy to the system, or achieve a given temperature in the reboiler. Finally, the cooling water flowrate, inlet temperature and permissible temperature rise are assigned in order to specify a desired condensate temperature or a given condenser duty. The validation of the proposed desorber model is performed by comparison of the model predictions of the liquid phase temperature profile with experimental data presented by Tobiesen *et al.* [77]. The predicted liquid phase temperature profiles in the desorber column are in reasonably good agreement with the experimental data and show the same linear temperature profile as the temperature profiles presented by Tobiesen *et al.* [77]. Some results for this process presented in figure 18. In order to validate the energetic aspects of our desorber model, we compare the reboiler duty and the extent of solvent regeneration obtained by supplying steam to the reboiler in order to obtain a desired reboiler temperature. In order to obtain the experimental reboiler temperature set point of 119.5°C, the model required that 10.5kW of energy be supplied which achieved a lean loading of 0.25 moles of CO<sub>2</sub> per mole of amine. These results compare well with the reported values of 9.6kW to obtain a lean loading of 0.24 moles of CO<sub>2</sub> per mole of amine. It is noted that due to the elevated temperatures at which the solvent regeneration process operates, the assumption of reaction equilibrium is well accepted here. On this basis, we consider the desorption process to be adequately validated and that we now have a suitable platform for carrying out process performance indexed solvent design studies.

### 3.2.2 Initial solvent design study

Solvent blends, particularly those including sterically hindered compounds, are considered to be an attractive approach to developing solvents for CO<sub>2</sub> capture. Recently, blends of AMP (a slow amine) and NH<sub>3</sub> have been shown to be particularly promising when compared to a standard 30wt% MEA solvent [78,79]. Specifically, this blend was presented as having reaction kinetics as fast as an MEA solvent, but with a significantly superior capacity for absorbing CO<sub>2</sub>. A 30wt% AMP + 5wt% NH<sub>3</sub> blend, denoted 30:5, has been suggested as promising. Our objective is to use the proposed model to identify an improved blend. To this end, we formulate an objective

function as follows:

$$f_{Obj} = Ay_{CO_2} + By_{RNH_2} + LCp \quad (17)$$

where  $A$ ,  $B$  are weights, with  $A=6,000$  and  $B=8,500$ ;  $y_{CO_2}$  is the outlet mole fraction of  $CO_2$  in the flue gas,  $y_{RNH_2}$  is the total outlet mole fraction of amine in the flue gas (i.e., the sum of the mole fractions of AMP and  $NH_3$ );  $L$  is the flow rate of the rich solvent stream leaving the absorption column in units of kmol/s;  $C_p$  is the heat capacity of that stream in units of kJ/kmol.K. The first term is related to the emission of  $CO_2$  to the atmosphere, the second to the emission of amine, and the third to the regeneration cost expressed in terms of the total heat capacity of the rich solvent stream. A solvent design problem has been solved on the basis of the proposed objective function using the inlet temperature,  $T$ , and composition,  $x_{NH_3}$  and  $x_{AMP}$  of the lean solvent stream and the flowrate  $L$  as design variables. The constraints include a minimum water content of 50wt% for the lean solvent, to avoid corrosion problems due to the presence of AMP. The results of the optimisation are compared to the best performance that can be achieved with the 30:5 blend, and are presented in figure 19. The optimal solvent blend has an increased AMP content and a decreased  $NH_3$  content, a greater solvent flow rate, and a reduced inlet temperature. Its performance in terms of separation effectiveness is similar to that of MEA: the mole fraction of  $CO_2$  in the flue gas ( $y_{CO_2}$ ) is 0.004 for MEA and 0.009 with the optimal blend. Given these promising results, a more realistic objective function must now be developed, to account in more detail for the compromise between absorption effectiveness and regeneration cost and to incorporate additional costs such as cooling the solvent to the desired inlet temperature.

## 4 Conclusions

In this project, we have developed detailed molecular thermodynamic models for a range of compounds of relevance to  $CO_2$  capture applications from coal-fired power-stations. These thermodynamic models have been incorporated in a rigorous process model of a  $CO_2$  capture process, whose performance has been validated using published pilot plant data for a range of solvents and operating conditions. Finally, some preliminary solvent design work has been completed, with blends of AMP and  $NH_3$  having been identified as promising solvents for  $CO_2$  capture. A significant part of this work has been the development of a novel approach for

modelling reactive separation processes, which makes the solution of solvent design problems for these systems much more tractable.

## 5 Proposed work for a subsequent programme

The models developed in this project have accurately accounted for fluid phase reactions in the case where there was only one reaction to consider, i.e., that between the amine and the CO<sub>2</sub>. However, in real operations, it is possible that there will be multiple acidic components in a flue gas, e.g., H<sub>2</sub>S and/or SO<sub>x</sub>. It would be of interest to investigate the suitability of the techniques developed in this work to date to dealing with processes involving multiple, parallel reactions.

Further, an area which is now ready for investigation is detailed solvent design activities, using a performance index linked to the performance of the entire CO<sub>2</sub> capture process. It is possible to identify solvent blends that minimise energy consumption or other objective functions. Additional research could also lead to the computer-aided design of novel solvent molecules. However, one property which is currently beyond the reach of our models is the susceptibility of amines to oxidative and other degradation. It is suggested that any rational solvent design procedure should accurately account for this phenomenon. It would therefore be of interest to develop a detailed, mechanistic understanding of the processes leading to solvent degradation, and incorporate this in future, process performance indexed solvent design activities.

## 6 Publications arising from the project

The following conference presentations and journal papers have been produced as a result of the work done in this project.

### Journal articles:

N. Mac Dowell, F. Llovel, C. S. Adjiman, G. Jackson, A. Galindo “Modelling the phase behaviour of the CO<sub>2</sub> + H<sub>2</sub>O + MEA mixture using transferable parameters with the SAFT-VR approach”, Accepted, Industrial and Engineering Chemistry Research, 2009



N. Mac Dowell, F. Llovel, A. Galindo, C. S. Adjiman, G. Jackson “Modelling the phase behaviour of  $\text{CO}_2 + \text{H}_2\text{O} + \text{RNH}_2$  mixtures with the SAFT-VR approach: a platform for solvent design”, To be submitted to Journal of Physical Chemistry B

F. Llovel, N. Mac Dowell, A. Galindo, F. Blas, G. Jackson “Study and prediction of interfacial properties of complex binary mixtures by means of a density functional theory based on the SAFT-VR equation of state”, To be submitted to Fluid Phase Equilibria

N. Mac Dowell, A. Galindo, C. S. Adjiman, G. Jackson “Modelling and design of MEA-based  $\text{CO}_2$  capture processes: Combining advanced thermodynamics and rate-based models”, To be submitted to Chemical Engineering Science

N. Mac Dowell, A. Galindo, C. S. Adjiman, G. Jackson “Modelling and design of AMP-based  $\text{CO}_2$  capture processes: Combining advanced thermodynamics and rate-based models”, For submission to Energy and Fuels, In preparation

N. Mac Dowell, A. Galindo, C. S. Adjiman, G. Jackson “An integrated process and solvent design platform for  $\text{CO}_2$  capture from low pressure gas”, For submission to AIChE Journal, In preparation

N. Mac Dowell, F. Llovel, A. Galindo, C. S. Adjiman, G. Jackson “On the modelling of multifunctional molecules using transferable parameters with the SAFT-VR approach”, For submission to Fluid Phase Equilibria, In preparation

N. Mac Dowell, A. Galindo, C. S. Adjiman, G. Jackson, Buchard, A. P, Williams, C., Hallett, J., Welton, T. and P. Fennell, “An overview of carbon capture technologies: State of the art and future perspectives”, To be submitted to Energy and Environmental Science

**Conference presentations:**

N. Mac Dowell, C. S. Adjiman, A. Galindo, G. Jackson, “Towards integrated solvent and process

design in amine-based processes for post-combustion CO<sub>2</sub> capture” (talk), The International Conference on Coal Science and Technology (ICCST), 28<sup>th</sup> - 31<sup>st</sup> August 2007, Nottingham University, Nottingham, UK

N. Mac Dowell, C. S. Adjiman, A. Galindo, G. Jackson, “Thermodynamic modelling of amine solvents” (poster), Thermodynamics 2007, 26<sup>th</sup>-28<sup>th</sup> September 2007, IFP, Rueil-Malmaison, Paris, France

N. Mac Dowell, C. S. Adjiman, A. Galindo, G. Jackson, “Improvements in amine flue gas scrubbing systems for coal fired power stations” (talk), British Coal Utilisation Research Association, Coal Research Forum (BCURA CRF) 4<sup>th</sup> June, 2008, Imperial College London, London, UK

N. Mac Dowell, C. S. Adjiman, A. Galindo, G. Jackson, “Modelling CO<sub>2</sub> capture in amine solvents with an advanced association model: Process optimisation and a platform for solvent design” (talk), American Institute for Chemical Engineers (AIChE) 2008 Annual meeting, 16<sup>th</sup>-21<sup>st</sup> November 2008, Philadelphia, USA

N. Mac Dowell, C. S. Adjiman, A. Galindo, G. Jackson, “Amine flue gas scrubbing systems: Integrating advanced thermodynamic modelling with sophisticated process simulation - an optimisation platform” (poster), UK Carbon Capture and Storage Consortium (UKCCSC) meeting, 24<sup>th</sup> November 2008, IMechE, London, UK

N. Mac Dowell, C. S. Adjiman, A. Galindo, G. Jackson, “Advanced thermodynamic and process modelling: Integration for amine scrubbing in post-combustion CO<sub>2</sub> capture” (poster), Imperial/Nature virtual conference on Climate Change and CO<sub>2</sub> Storage, Dec. 3, 2008, Available from Nature Precedings <http://dx.doi.org/10.1038/npre.2008.2638.1> (2008)

N. Mac Dowell, C. S. Adjiman, A. Galindo, G. Jackson, “Model based optimisation of a multicomponent chemisorption process for CO<sub>2</sub> capture: A solvent design platform” (talk), The 5<sup>th</sup> Trondheim Conference on CO<sub>2</sub> Capture, Transport and Storage, 16-17 June, 2009, NTNU, Trondheim, Norway

N. Mac Dowell, F. Llovell, C. S. Adjiman, A. Galindo, G. Jackson, “Transferable association models of amine + CO<sub>2</sub> + H<sub>2</sub>O mixtures using the SAFT-VR approach” (poster), Thermodynamics 2009, 23-25th September 2009, Imperial College London, London, UK

F. Llovell, N. Mac Dowell, G. Jackson, A. Galindo, F. J. Blas “Development of an accurate SAFT-VR-DFT equation of state for the prediction of interfacial properties of complex mixtures” (short talk + poster), Thermodynamics 2009, 23-25th September 2009, Imperial College London, London, UK

F. Llovell, N. Mac Dowell, G. Jackson, A. Galindo, F. J. Blas “A DFT formalism combined with the SAFT-VR equation of state for the prediction of interfacial phenomena” (poster), XVI Congreso de Física Estadística, Huelva, Spain, 10<sup>th</sup>- 12<sup>th</sup> September 2009

N. Mac Dowell, C. S. Adjiman, A. Galindo, G. Jackson, “Modelling and design of MEA-based CO<sub>2</sub> capture processes: Combining advanced thermodynamics and rate-based models” (talk), American Institute for Chemical Engineers (AIChE) 2009 Annual meeting, 8<sup>th</sup>- 13<sup>th</sup> November 2009, Nashville, USA

N. Mac Dowell, C. S. Adjiman, A. Galindo, G. Jackson, “An integrated process and solvent design platform for CO<sub>2</sub> capture from low pressure gas” (talk), American Institute for Chemical Engineers (AIChE) 2009 Annual meeting, 8<sup>th</sup>- 13<sup>th</sup> November 2009, Nashville, USA

N. Mac Dowell, C. S. Adjiman, A. Galindo, G. Jackson, “Modelling the phase behaviour of the CO<sub>2</sub> + H<sub>2</sub>O + Amine mixtures using transferable parameters with SAFT-VR” (talk), American Institute for Chemical Engineers (AIChE) 2009 Annual meeting, 8<sup>th</sup>- 13<sup>th</sup> November 2009, Nashville, USA

N. Mac Dowell, A. Galindo, G. Jackson, C. S. Adjiman, “Integrated solvent and process design for the reactive separation of CO<sub>2</sub> from flue gases” (talk), ESCAPE-20, European Symposium on Computer Aided Process Engineering, 6<sup>th</sup>-9<sup>th</sup> June, 2010, Naples, Italy

N. Mac Dowell, A. Galindo, G. Jackson, C. S. Adjiman, “The integrated design of solvent blends and separation processes for CO<sub>2</sub> capture from flue gases” (talk), PPEPPD-12, Properties and Phase Equilibria for Product and Process Design, May 16<sup>th</sup> - 21<sup>st</sup>, 2010, Suzhou, Jiangsu, China

F. Llovel, N. Mac Dowell, G. Jackson, A. Galindo, F. J. Blas “Fundamentals, development and application of DFT theories to a SAFT-type equation of state for the prediction of interfacial phenomena in complex mixtures” (talk), PPEPPD-12, Properties and Phase Equilibria for Product and Process Design, May 16<sup>th</sup> - 21<sup>st</sup>, 2010, Suzhou, Jiangsu, China

## References

- [1] Meeting the energy challenge A white paper on energy. Technical report, Department of Trade and Industry, May 2007. [www.berr.gov.uk/files/file39387.pdf](http://www.berr.gov.uk/files/file39387.pdf).
- [2] IPCC. Intergovernmental panel on climate change, third assessment report. Technical report, IPCC, 2001.
- [3] B. Metz, O. Davidson, H. C. de Coninck, M. Loos, and L. A. Meyer. *IPCC, 2006: IPCC Special Report of Carbon Dioxide Capture and Storage. Prepared by Working Group III of the Intergovernmental Panel on Climate Change*. Cambridge University Press, Cambridge, United Kingdom and New York, NY, USA, 2005.
- [4] J. H. St Clair and W. F. Simister. Process to recover CO<sub>2</sub> from flus gas gets first large scale tryout in Texas. *Oil Gas J.*, 6:109–113, 1983.
- [5] A. B. Rao and E. S. Rubin. A technical, economic and enviromental assessment of amine-based CO<sub>2</sub> capture technology for power plant greenhouse gas control. *Environ. Sci. Technol.*, 36(20):4467–4475, 2002.
- [6] G. Astarita, D. W. Savage, and A. Bisio. *Gas Treating With Chemical Solvents*. John Wiley and Sons, New York, 1983.
- [7] A. M. Wolsky, E. J. Daniels, and B. J. Jody. CO<sub>2</sub> capture from the flue gas of conventional fossil fuel fired power plants. *Environ. Prog.*, 13:214–219, 1994.
- [8] A. Giovanoglou, J. Barlatier, C. S. Adjiman, E. N. Pistokopoulos, and J. L. Cordiner. Optimal solvent design for batch separation based on economic performance. *AIChE J.*, 49(12):3095–3109, 2003.
- [9] L. Kucka, I. Muller, E. Y. Kenig, and A. Gorak. On the modelling and simulation of sour gas absorption by aqueous amine solutions. *Chem. Eng. Sci.*, 58(16):3571–3578, 2003.
- [10] W. P. M. van Swaaij and G. F. Versteeg. Mass transfer accompanied with complex reversible chemical reactions in gas-liquid systems: An overview. *Chem. Eng. Sci.*, 47(13–14):3181–3195, 1992.
- [11] W. J. DeCoursey. Enhancement factors for gas absorption with reversible reaction. *Chem. Eng. Sci.*, 37(10):1483–1489, 1982.
- [12] W. J. DeCoursey and R. W. Thring. Effects of unequal diffusivities on enhancement factors for reversible and irreversible reaction. *Chem. Eng. Sci.*, 44(8):1715–1721, 1989.
- [13] A. Gil-Villegas, A. Galindo, P.J. Whitehead, S.J. Mills, and G Jackson. Statistical associating fluid theory for chain molecules with attractive potentials of variable range. *J.*

- Chem. Phys.*, 106(10), 1997.
- [14] A. Galindo, L.A. Davies, Gil-Villegas, and G. Jackson. The thermodynamics of mixtures and the corresponding mixing rules in the SAFT-VR approach for potentials of variable range. *Mol. Phys.*, 93(2):241–252, 1998.
- [15] G. Astarita. *Mass Transfer With Chemical Reaction*. Elsevier, London, 1967.
- [16] H. Hikita, S. Asai, H. Ishikawa, and M. Honda. The kinetics of reactions of carbon dioxide with monoethanolamine, diethanolamine and triethanolamine by a rapid mixing method. *Chem. Eng. J.*, 13(1):7–12, 1977.
- [17] P. V. Danckwerts. The reaction of CO<sub>2</sub> with ethanolamines. *Chem. Eng. Sci.*, 34(4):443–446, 1979.
- [18] S. S. Laddha and P. V. Danckwerts. Reaction of CO<sub>2</sub> with ethanolamines: kinetics from gas-absorption. *Chem. Eng. Sci.*, 3(36):479–482, 1981.
- [19] D.E. Penny and T.J. Ritter. Kinetic study of the reactions between carbon dioxide and primary amines. *J. Chem. Soc., Faraday Trans. I.*, 79:2103–2109, 1983.
- [20] P.M.M. Blauwhoff, G.F. Versteeg, and W.P.M. van Swaaij. A study on the reaction between CO<sub>2</sub> and alkanolamines in aqueous solutions. *Chem. Eng. Sci.*, 39(2):207–225, 1984.
- [21] L. Faramarzi, G. M. Kontogeorgis, K. Thomsen, and E. H. Stenby. Extended UNIQUAC model for thermodynamic modelling of CO<sub>2</sub> absorption in aqueous alkanolamine solutions. *Fluid Phase Equilib.*, 282:121–132, 2009.
- [22] G. Maurer. Phase equilibria in chemically reactive systems. *Fluid Phase Equilib.*, 30:337–352, 1986.
- [23] G. Maurer. Phase equilibria in chemical reactive fluid mixtures. *Fluid Phase Equilib.*, 116:39–51, 1996.
- [24] J.M. Prausnitz, R.N. Lichtenthaler, and E.G. de Azevedo. *Molecular thermodynamics of fluid phase equilibria*. Prentice Hall, 1999.
- [25] E. A. Guggenheim. The statistical mechanics of regular solutions. *Proc. R. Soc. Lond., Series A*, 148(864):304–312, 1935.
- [26] E. A. Guggenheim. The statistical mechanics of co-operative assemblies. *Proc. R. Soc. Lond. A*, 169(936):134–148, 1938.
- [27] G. S. Rushbrooke. A note on Guggenheim’s theory of strictly regular binary liquid mixtures. *Proc. R. Soc. Lond. A*, 166(925):296–315, 1938.

- [28] E. A. Guggenheim. *Mixtures*. Clarendon Press, Oxford, 1952.
- [29] C. C. Chen, H. I. Britt, J. F. Boston, and L. B. Evans. Local composition model for excess Gibbs energy of electrolyte systems. Part I: Single solvent, single completely dissociated electrolyte systems. *AIChE J.*, 28(3):588–596, 1982.
- [30] C. C. Chen and L. B. Evans. A local composition model for the excess Gibbs energy of aqueous electrolyte systems. *AIChE J.*, 32(3):444–454, 1986.
- [31] H. Renon and J. M. Prausnitz. Local compositions in thermodynamic excess functions for liquid mixtures. *AIChE J.*, 14(1):135–144, 1968.
- [32] G. Soave. Equilibrium constants from a modified Redlich-Kwong equation of state. *Chemical Engineering Science*, 1972.
- [33] H. M. Kvamsdal, J. P. Jakobsen, and K. A. Hoff. Dynamic modelling and simulation of a CO<sub>2</sub> absorber column for post-combustion CO<sub>2</sub> capture. *Chem. Eng. Proc.*, 48(1):135–144, 2009.
- [34] S. Ziaii, G. T. Rochelle, and T. F. Edgar. Dynamic modeling to minimize energy use for CO<sub>2</sub> capture in power plants by aqueous monoethanolamine. *Ind. Eng. Chem. Res.*, 48(13):6105–6111, 2009.
- [35] J. Gabrielsen, M. L. Michelsen, E. H. Stenby, and G. M. Kontogeorgis. A model for estimating CO<sub>2</sub> solubility in aqueous alkanolamines. *Ind. Eng. Chem. Res.*, 44:3348–3354, 2005.
- [36] A. Aboudheir, P. Tontiwachwuthikul, A. Chakama, and R. Idem. Kinetics of the reactive absorption of carbon dioxide in high CO<sub>2</sub> loaded concentrated aqueous monoethanolamine solutions. *Chem. Eng. Sci.*, 58:5195–5210, 2003.
- [37] J. Gabrielsen, M. L. Michelsen, E. H. Stenby, and G. M. Kontogeorgis. Modeling of CO<sub>2</sub> absorber using an AMP solution. *AIChE J.*, 52(10):3443–3451, 2006.
- [38] D. deMontigny, A. Aboudheir, and P. Tontiwachwuthikul. Modelling the performance of a CO<sub>2</sub> absorber containing structured packing. *Ind. Eng. Chem. Res.*, 45(8):2594–2600, 2006.
- [39] R. Dohrn and O. Pfohl. Thermophysical properties - Industrial directions. *Fluid Phase Equilib.*, 194–197:15–29, 2002.
- [40] P. Paricaud, A. Galindo, and G. Jackson. Recent advances in the use of the SAFT approach in describing electrolytes, interfaces, liquid crystals and polymers. *Fluid Phase Equilibria*, 194–197:87–96, 2002.

- [41] S. P. Tan, H. Adidharma, and M. Radosz. Recent advances and applications of statistical associating fluid theory. *Ind. Eng. Chem. Res.*, 47(21):8063–8082, 2008.
- [42] R. Taylor and R. Krishna. *Multicomponent Mass Transfer*. Wiley, 1993.
- [43] E. Y Kenig, R. Schneider, and A Gorak. Reactive absorption: Optimal process design via optimal modelling. *Chem. Eng. Sci.*, 56(2):343–350, 2001.
- [44] R. Krishnamurthy and R. Taylor. A nonequilibrium stage model of multicomponent separation processes, Part I: Model description and method of solution. *AIChE J.*, 31(3):449–456, 1985.
- [45] W. K. Lewis and W. G. Whitman. Principles of gas absorption. *Ind. Eng. Chem.*, 16(12):1215–1220, 1924.
- [46] S. Hatta. On the absorption velocity of gases by liquids. *Technical Reports from Tohoku Imperial University*, 10:119–135, 1932.
- [47] R. E. Treybal. Adiabatic gas absorption and stripping in packed towers. *Ind. Eng. Chem.*, 61(7):36–41, 1969.
- [48] J. D. Pandya. Adiabatic gas absorption and stripping with chemical reaction in packed towers. *Chem. Eng. Commun.*, 19:343–361, 1982.
- [49] P. Tontiwachwuthikul, A. Meisen, and Lim C. J. CO<sub>2</sub> absorption by NaOH, monoethanolamine and 2-amino-2-methyl-1-propanol solutions in a packed column. *Chem. Eng. Sci.*, 47(2):381–390, 1992.
- [50] E.Y. Kenig, R. Schneider, and A. Gorak. Rigorous dynamic modelling of complex reactive absorption processes. *Chem. Eng. Sci.*, 54(21):5195–5203, 1999.
- [51] J. C. Charpentier. *Multiphase chemical reactors Volume II - Design methods*, chapter General characteristics of multiphase gas-liquid reactors: Hydrodynamics and mass transfer, pages 157–270. Alphen aan den Rijn, The Netherlands, 1981.
- [52] A. E. Rodrigues, J. M. Calo, and N. H. Sween, editors. *Multiphase Chemical Reactors Volume I - Fundamentals*. Nato Advanced Study Institutes Series, 1980.
- [53] A. E. Rodrigues, J. M. Calo, and N. H. Sween, editors. *Multiphase Chemical Reactors Volume II - Design Methods*. Nato Advanced Study Institutes Series, 1980.
- [54] R. B. Bird, W. E. Stewart, and E. N. Lightfoot. *Transport Phenomena*. Wiley, second edition, 2007.
- [55] G. Jackson, W. G. Chapman, and K. E. Gubbins. Phase equilibria of associating fluids spherical molecules with multiple bonding sites. *Mol. Phys.*, 65(1):1–31, 1988.



- [56] H. Thompson, J.C. Wasse, N.T. Skipper, C.A. Howard, D.T. Bowron, and A.K. Soper. The structure of polaronic electron cavities in lithium-ammonia solutions. *J. Phys.: Condens. Matter*, 16:5639–5652, 2004.
- [57] G. N. I. Clark, A. J. Haslam, A. Galindo, and G. Jackson. Developing optimal Wertheim-like models of water for use in statistical associating fluid theory (SAFT) and related approaches. *Mol. Phys.*, 104(22–24), 2006.
- [58] J. S. Rowlinson and F. L Swinton. *Liquids and Liquid Mixtures*. Butterworth - Heinmann, London, Third edition, 1982.
- [59] PSE, 2007. <http://www.psenterprise.com/>.
- [60] K. P. Resnik, J. T. Yeh, and H. W. Pennline. Aqua ammonia process for simultaneous removal of CO<sub>2</sub>, SO<sub>2</sub> and NO<sub>x</sub>. *Int. J. of Environmental Technology & Management*, 4(1/2):89–104, 2004.
- [61] R. Peltier. Alstom’s chilled ammonia CO<sub>2</sub> capture process advances toward commercialisation. *Power*, 2008. Available from: [www.powermag.com/environmental/Alstoms chilled ammonia CO2 capture process advances toward commercialization 86 p4.html](http://www.powermag.com/environmental/Alstoms%20chilled%20ammonia%20CO2%20capture%20process%20advances%20toward%20commercialization%2086%20p4.html).
- [62] Chilling news for carbon capture. *Mod. Power Syst.*, 26(12):17–18, 2006.
- [63] A. C. Larsson. The chilled ammonia process by ALSTOM - Status of development. In *The 5<sup>th</sup> Trondheim conference on CO<sub>2</sub> capture, transport and storage*, 2009. Available from: [www.energy.sintef.no/arr/CO2/2009/Presentations/A6-1.pdf](http://www.energy.sintef.no/arr/CO2/2009/Presentations/A6-1.pdf).
- [64] U. Goppert and G. Maurer. Vapour - liquid equilibria in aqueous solutions of ammonia and carbon dioxide at temperatures between 333 and 393 K and pressures up to 7 MPa. *Fluid Phase Equilib.*, 41(1–2):153–185, 1988.
- [65] N. Mac Dowell, F. Llovel, C. S. Adjiman, G. Jackson, and A. Galindo. Modelling the fluid phase behaviour of carbon dioxide in aqueous solutions of monoethanolamine using transferable parameters with the SAFT-VR approach. *Ind. Eng. Chem. Res. (Accepted)*, 2009.
- [66] A. Galindo, P. J. Whitehead, G. Jackson, and A. N. Burgess. Predicting the high-pressure phase equilibria of water + n-alkanes using a simplified SAFT theory with transferable intermolecular interaction parameters. *J. Phys. Chem.*, 100(16):6781–6792, 1996.
- [67] G. N. I. Clark, A. Galindo, G. Jackson, S. Rogers, and A. N. Burgess. Modeling and understanding closed-loop liquid-liquid immiscibility in aqueous solutions of poly(ethylene glycol) using the SAFT-VR approach with transferable parameters. *Macromolecules*, 41(17):6582–6595, 2008.

- [68] D. Hopfe. Thermophysical data of pure substances. *Data Compilation of Fiz Chemie Germany*, 1990.
- [69] G. Vazquez, E. Alvarez, J. M. Navaza, R. Rendo, and E. Romero. Surface tension of binary mixtures of water + monoethanolamine and water + 2-amino-2-methyl-1-propanol and tertiary mixtures of these amines with water from 25 C to 50 C. *J. Chem. Eng. Data*, 42(1):57–59, 1997.
- [70] K. Moerke and T. Roscher. Determination of the surface tension of some ethyleneamines. *Leuna protocol*, 1982.
- [71] G. Liessmann, W. Schmidt, and S. Reiffarth. Recommended thermophysical data. *Data compilation of the Saechsische Olefinwerke Boehlen Germany*, 1995.
- [72] J. I Lee, F. D. Otto, and A. E. Mather. Equilibrium between carbon dioxide and aqueous monoethanolamine solutions. *J. Appl. Biotechnol.*, 26(10):541–549, 1976.
- [73] F. Y Jou, A. E. Mather, and F. D. Otto. The solubility of CO<sub>2</sub> in a 30 mass percent monoethanolamine solution. *Can J. Chem. Eng.*, 73(1):140–147, 1995.
- [74] R. Dugas. Pilot plant study of carbon dioxide capture by aqueous monoethanolamine. Master’s thesis, The University of Texas at Austin, 2006.
- [75] N. M. P. Kakalis, A. I. Kakhu, and C. C. Pantelides. Efficient solution of the association term equations in the statistical associating fluid theory equation of state. *Ind. Eng. Chem. Res.*, 45(17):6056–6062, 2006.
- [76] R. Taylor. (Di)Still modelling after all these years: A view of the state of the art. *Ind. Eng. Chem. Res.*, 46(13):4349–4357, 2007.
- [77] F. A. Tobiesen, O. Juliussen, and H. F. Svendsen. Experimental validation of a rigorous desorber model for CO<sub>2</sub> postcombustion capture. *Chem. Eng. Sci.*, 63:2641–2656, 2008.
- [78] W. J. Choi, B. M. Min, B. H. Shon, J. B. Seo, and K. J. Oh. Characteristics of absorption/regeneration of CO<sub>2</sub>-SO<sub>2</sub> binary systems into aqueous AMP+ammonia solutions. *J. Ind. Eng. Chem.*, 2009. In Press.
- [79] W. J. Choi, J. B. Seo, S. Y. Jang, J. H. Jung, and W. J. Oh. Removal characteristics of CO<sub>2</sub> using aqueous AME/AMP solutions in the absorption and regeneration process. *J. Env. Sci.*, 21:907–913, 2009.
- [80] D. A. Fletcher, R. F. McMeeking, and D. Parkin. The United Kingdom Chemical Database Service. *J. Chem. Inf. Comput. Sci.*, 36(4):746–749, 1996.

- [81] D. Silkenbaeumer, B. Rumpf, and R. N. Lichtenthaler. Solubility of carbon dioxide in aqueous solutions of 2-amino-2-methyl-1-propanol and n-methyldiethanolamine and their mixtures in the temperature range from 313 to 353 K and pressures up to 2.7 MPa. *Ind. Eng. Chem. Res.*, 38(8):3133–3141, 1988.

## List of Figures

- 1 Experimental data (squares) [80] for the pressure-temperature ( $PT$ ) phase diagram of  $\text{NH}_3$ , AMP and MEA are compared with the SAFT-VR description for the SAFT-VR models (continuous curves). . . . . 39
- 2 Experimental data (squares) [80] for the vapour-liquid coexistence densities,  $\rho$  of  $\text{NH}_3$ , AMP and MEA are compared with the SAFT-VR description for the models of these molecules (continuous curves) . . . . . 40
- 3 a)Experimental data (squares) [80] for the enthalpy of vapourisation of  $\text{NH}_3$ ,  $\Delta H_{fg}^{\text{NH}_3}$ , are compared with the SAFT-VR description for the models of these molecules (continuous curves), b)Experimental data (squares) [80] for the vapour-liquid interfacial tension of  $\text{NH}_3$ ,  $\gamma^{\text{NH}_3}$ , are compared with the SAFT-VR description for the models of these molecules (continuous curves) . . . . . 41
- 4 Isotherms of the pressure-composition ( $P-x$ ) vapour-liquid equilibria of  $\text{NH}_3+\text{H}_2\text{O}$  compared with SAFT-VR models of  $\text{NH}_3$ . The symbols correspond to the experimental data at  $T=333.15\text{K}$  [80] and the curves to the corresponding SAFT-VR description. . . . . 42
- 5 Isothermal projection of the pressure-loading ( $P-x$ ) vapour-liquid equilibria of the ternary mixture of  $\text{NH}_3+\text{H}_2\text{O}+\text{CO}_2$ , where  $\theta$  is defined as  $x_{\text{CO}_2}/x_{\text{NH}_3}$ . The symbols correspond to the experimental data at  $T=333.15\text{K}$  and  $m_{\text{NH}_3} = 0.591$  [64] and the curves to the corresponding SAFT-VR description. This data set was used to obtain the  $\text{NH}_3+\text{CO}_2$  binary interaction parameters. . . . . 43
- 6 Isothermal projections of the pressure-composition ( $P-x$ ) vapour-liquid equilibria of the ternary mixture of  $\text{NH}_3+\text{H}_2\text{O}+\text{CO}_2$ , where  $\theta$  is defined as  $x_{\text{CO}_2}/x_{\text{NH}_3}$ . The symbols correspond to the experimental data at  $T=353.15\text{K}$  and  $m_{\text{NH}_3} = 0.591$  [64] and the curves to the corresponding SAFT-VR description. These results are a prediction, not a correlation. . . . . 44

- 7 Contour plot for the relative average absolute deviation (%AAD) of the vapour pressure and saturated liquid density determined using the SAFT-VR equation of state with the asymmetric model of MEA. At each point on the surface, the dispersion  $\varepsilon_{MEA}/k$  and self-cross-association  $\varepsilon_{eH,MEA}^{HB}/k$  and  $\varepsilon_{e^*H^*,MEA}^{HB}/k$  energies are fixed, and the size ( $\sigma_{MEA}$ ) and range ( $\lambda_{MEA}$ ) parameters are optimised by minimising the least-squares objective function for 376 points between the triple-point temperature to 90% of the critical point. The optimal model on this surface corresponds to %AAD  $P^{Sat} + \rho_l = 2.41\%$ . Only the relevant section of the entire parameter space explored is depicted. . . . . 45
- 8 Experimental data (squares) [80] for the enthalpy of vaporisation  $\Delta H_{vap}$  of MEA compared with SAFT-VR predictions for the asymmetric model (continuous curve). 46
- 9 Experimental data (squares) [80] for vapour-liquid interfacial tension of MEA compared with SAFT-VR predictions for the asymmetric model (continuous curve). 47
- 10 Isotherms of the pressure-composition ( $P-x$ ) vapour-liquid equilibria of MEA+H<sub>2</sub>O compared with SAFT-VR calculations with both the symmetric and asymmetric models of MEA. The continuous curves are the calculations with the asymmetric model of MEA and the dashed line curves those with the symmetric model of MEA. Three representative temperatures are shown:  $\square$ ,  $T = 298.15$  K;  $\circ$ ,  $T = 343.15$  K;  $\diamond$ ,  $T = 363.15$  K. The symbols correspond to the experimental data [80] and the curves to the corresponding SAFT-VR description. . . . . 48
- 11 Isothermal projections of the pressure-composition ( $Px$ ) vapour-liquid equilibria of the ternary mixture MEA+CO<sub>2</sub>+H<sub>2</sub>O compared with SAFT-VR description: a)  $T = 313.15$  K, b)  $T = 333.15$  K, and c)  $T = 353.15$  K. The thick continuous curves correspond to SAFT-VR calculations with the asymmetric model of MEA, and the thick dashed curve in a) to SAFT-VR calculations with the symmetric model of MEA. In all figures, the thin continuous curves corresponds to a correlation presented by Aboudheir *et al.* [36] and the thin dashed curve corresponds to a correlation presented by Gabrielsen *et al.* [35] The symbols denote the experimental data:  $\square$  correspond to the data of Jou and Mather [73];  $\diamond$  and  $\triangleright$  correspond to the data of Dugas [74];  $\circ$  correspond to the data of Lee *et al.* [72] 49

12	Binary VLE calculations for the AMP+H <sub>2</sub> O mixture compared with experimental data. The continuous lines correspond to SAFT-VR calculations and the symbols (□) to experimental data obtained from Pappa <i>et al.</i> [?] at a constant pressure of $P = 0.1\text{MPa}$ . . . . .	50
13	Ternary VLE calculations for the AMP+CO <sub>2</sub> +H <sub>2</sub> O mixture compared with experimental data. The continuous lines correspond to SAFT-VR calculations and the symbols (□) to the experimental data of [81] at a constant temperature of $T = 353.15\text{ K}$ . . . . .	51
14	Evolution of model complexity, taken from Kenig <i>et al.</i> [43] . . . . .	52
15	Representation of column stage . . . . .	52
16	a) Liquid phase temperature profile for absorber column, b) Gas phase CO <sub>2</sub> concentration profile for absorber column, c) Liquid phase CO <sub>2</sub> loading profile for absorber column. The continuous curves correspond to the predictions of our model, and the symbols correspond to pilot plant data obtained from run T22 in [49]. Stage 1 corresponds to the top of the column, and stage 25 to the bottom. An MEA solvent is used. . . . .	53
17	a) Liquid phase temperature profile for absorber column, b) Gas phase CO <sub>2</sub> concentration profile for absorber column, c) Liquid phase CO <sub>2</sub> loading profile for absorber column. The continuous curves correspond to the predictions of our model, and the symbols correspond to pilot plant data obtained from run T26 in [49]. Stage 1 corresponds to the top of the column, and stage 25 to the bottom. An AMP solvent is used. . . . .	54
18	Liquid phase temperature profile for NTNU desorber from [77]. The continuous curves correspond to the predictions of our model, and the symbols correspond to pilot plant data. Stage 1 corresponds to the top of the column, and stage 25 to the bottom. An MEA solvent is used. . . . .	55

19 Predicted temperature and composition profiles for an industrial scale absorption column a) Liquid phase temperature profile b) Gas phase CO<sub>2</sub> concentration profile c) Liquid phase CO<sub>2</sub> loading profile. The continuous curves correspond to a 30wt% MEA solvent, the dotted curves correspond to a 30wt% AMP + 5wt%NH<sub>3</sub> solvent blend and the dashed curves correspond to an optimised solvent blend comprising 37.7wt% AMP and 1.96wt% NH<sub>3</sub> mixture. . . . . 56

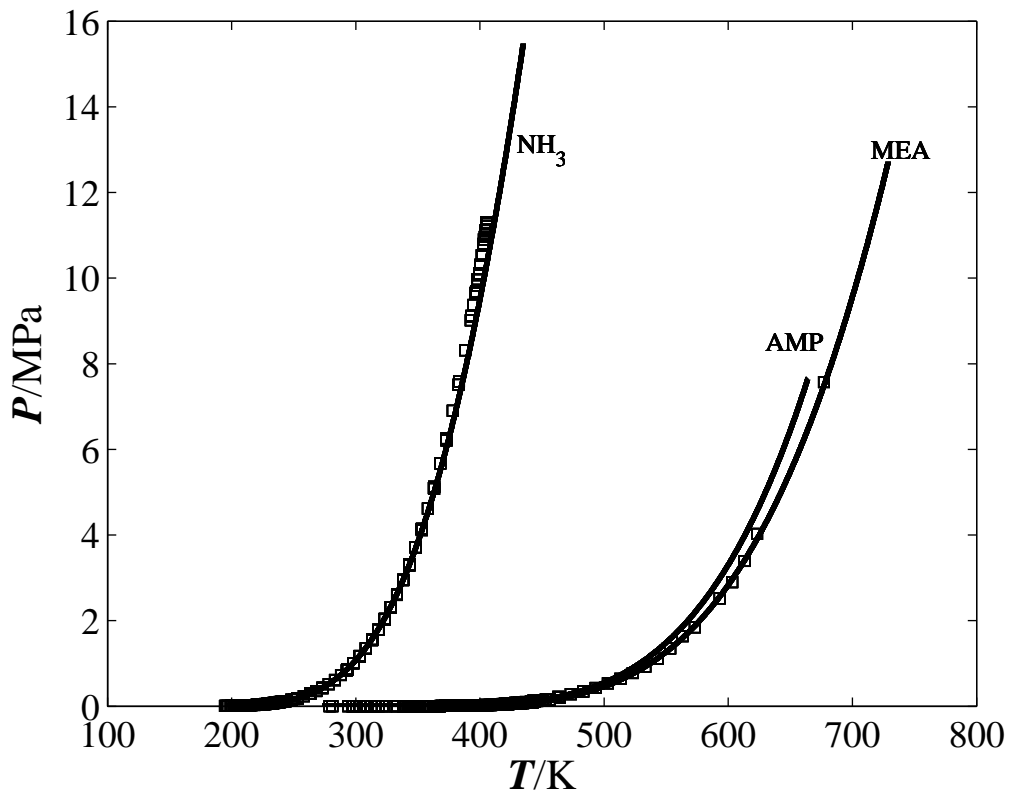


Figure 1: Experimental data (squares) [80] for the pressure-temperature ( $PT$ ) phase diagram of  $\text{NH}_3$ , AMP and MEA are compared with the SAFT-VR description for the SAFT-VR models (continuous curves).



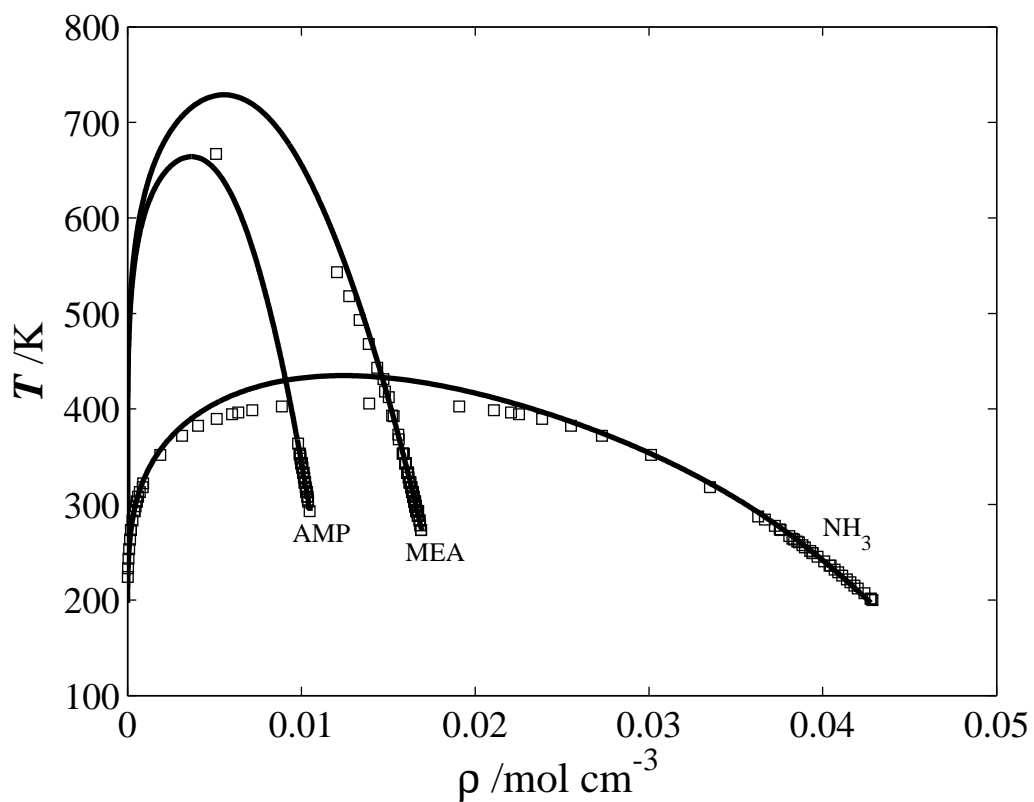


Figure 2: Experimental data (squares) [80] for the vapour-liquid coexistence densities,  $\rho$  of  $\text{NH}_3$ , AMP and MEA are compared with the SAFT-VR description for the models of these molecules (continuous curves)

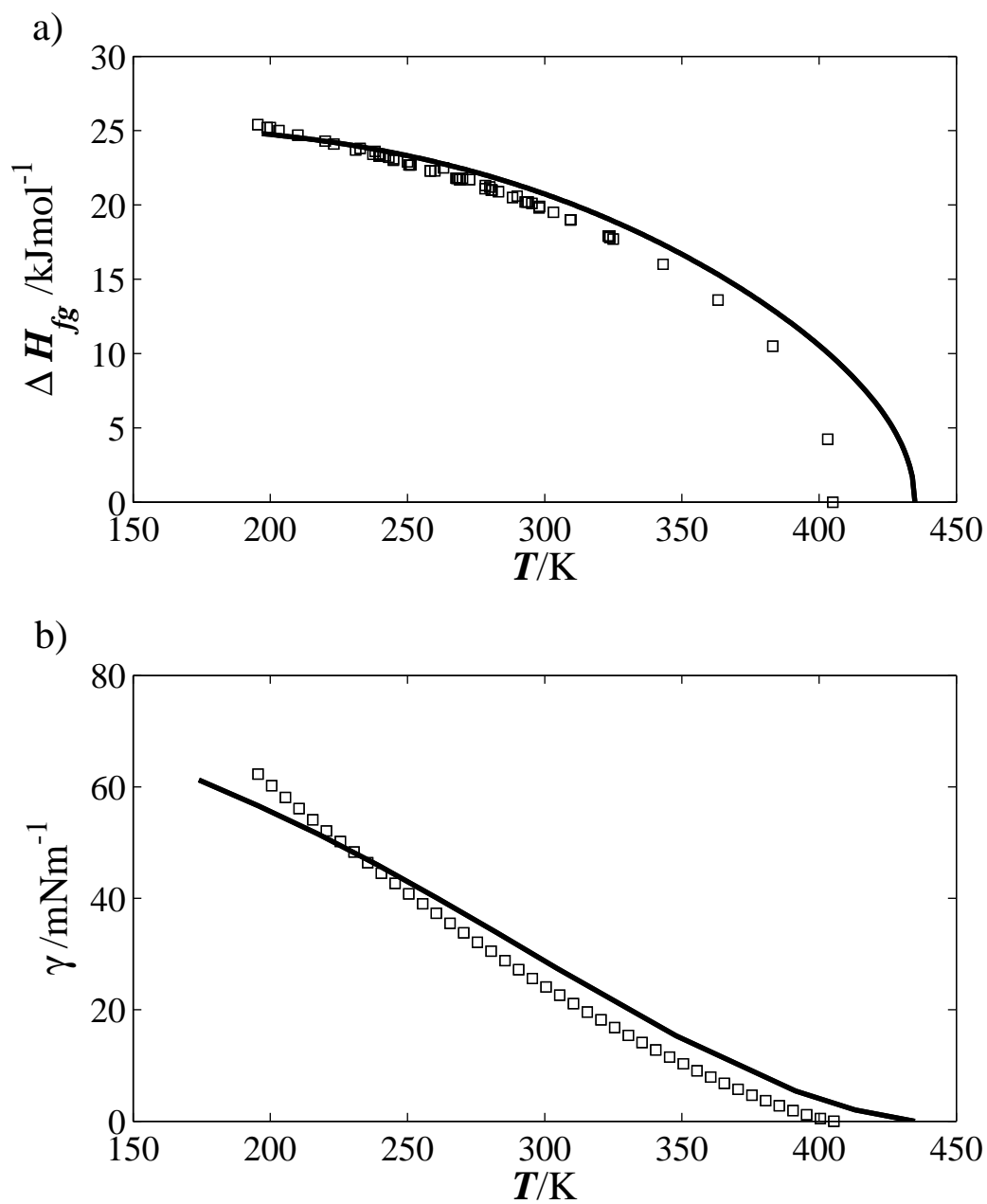


Figure 3: a) Experimental data (squares) [80] for the enthalpy of vapourisation of NH<sub>3</sub>,  $\Delta H_{fg}^{NH_3}$ , are compared with the SAFT-VR description for the models of these molecules (continuous curves), b) Experimental data (squares) [80] for the vapour-liquid interfacial tension of NH<sub>3</sub>,  $\gamma^{NH_3}$ , are compared with the SAFT-VR description for the models of these molecules (continuous curves)

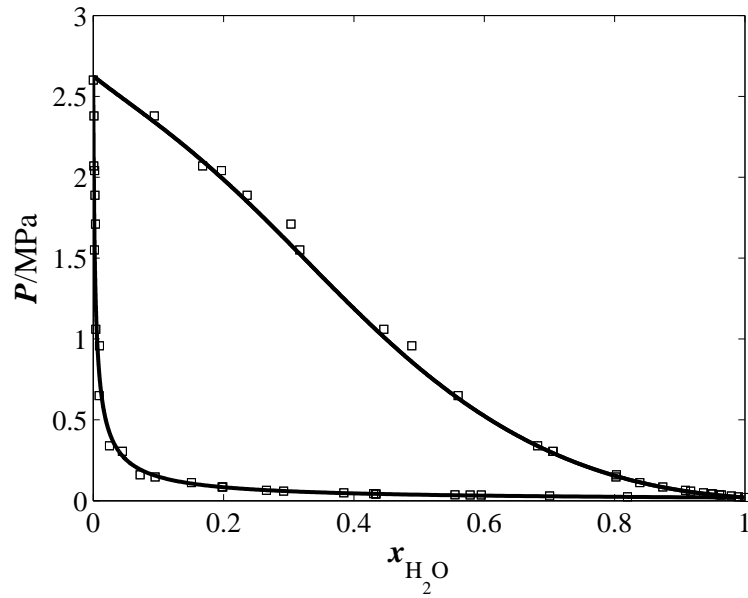


Figure 4: Isotherms of the pressure-composition ( $P - x$ ) vapour-liquid equilibria of  $\text{NH}_3 + \text{H}_2\text{O}$  compared with SAFT-VR models of  $\text{NH}_3$ . The symbols correspond to the experimental data at  $T = 333.15\text{K}$  [80] and the curves to the corresponding SAFT-VR description.

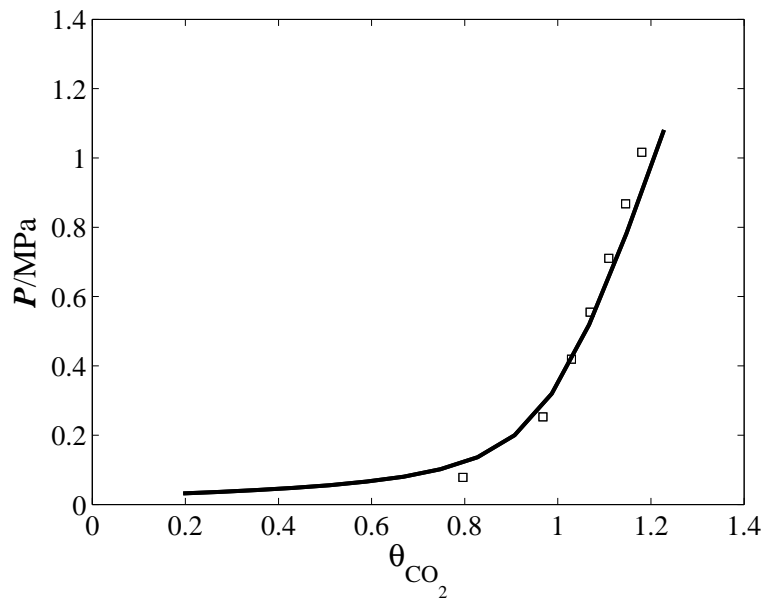


Figure 5: Isothermal projection of the pressure-loading ( $P - x$ ) vapour-liquid equilibria of the ternary mixture of  $NH_3+H_2O+CO_2$ , where  $\theta$  is defined as  $x_{CO_2}/x_{NH_3}$ . The symbols correspond to the experimental data at  $T=333.15K$  and  $m_{NH_3} = 0.591$  [64] and the curves to the corresponding SAFT-VR description. This data set was used to obtain the  $NH_3+CO_2$  binary interaction parameters.

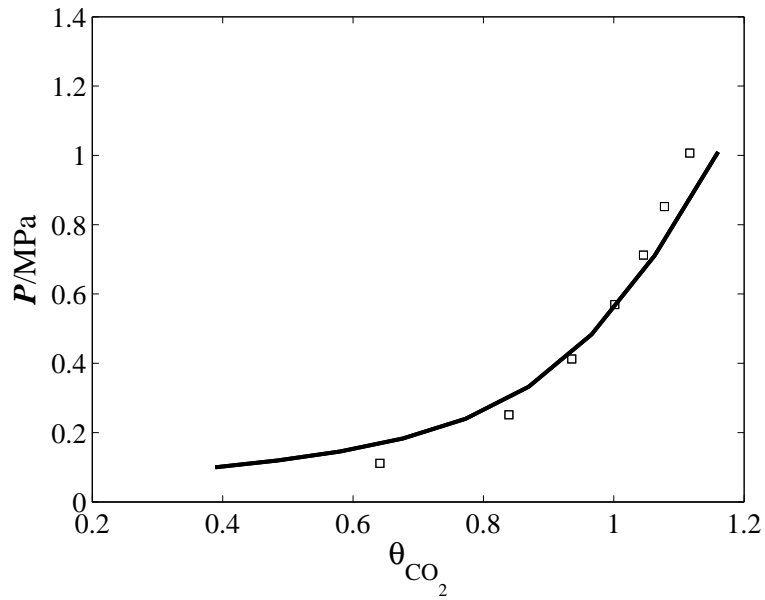


Figure 6: Isothermal projections of the pressure-composition ( $P - x$ ) vapour-liquid equilibria of the ternary mixture of  $\text{NH}_3 + \text{H}_2\text{O} + \text{CO}_2$ , where  $\theta$  is defined as  $x_{\text{CO}_2}/x_{\text{NH}_3}$ . The symbols correspond to the experimental data at  $T=353.15\text{K}$  and  $m_{\text{NH}_3} = 0.591$  [64] and the curves to the corresponding SAFT-VR description. These results are a prediction, not a correlation.

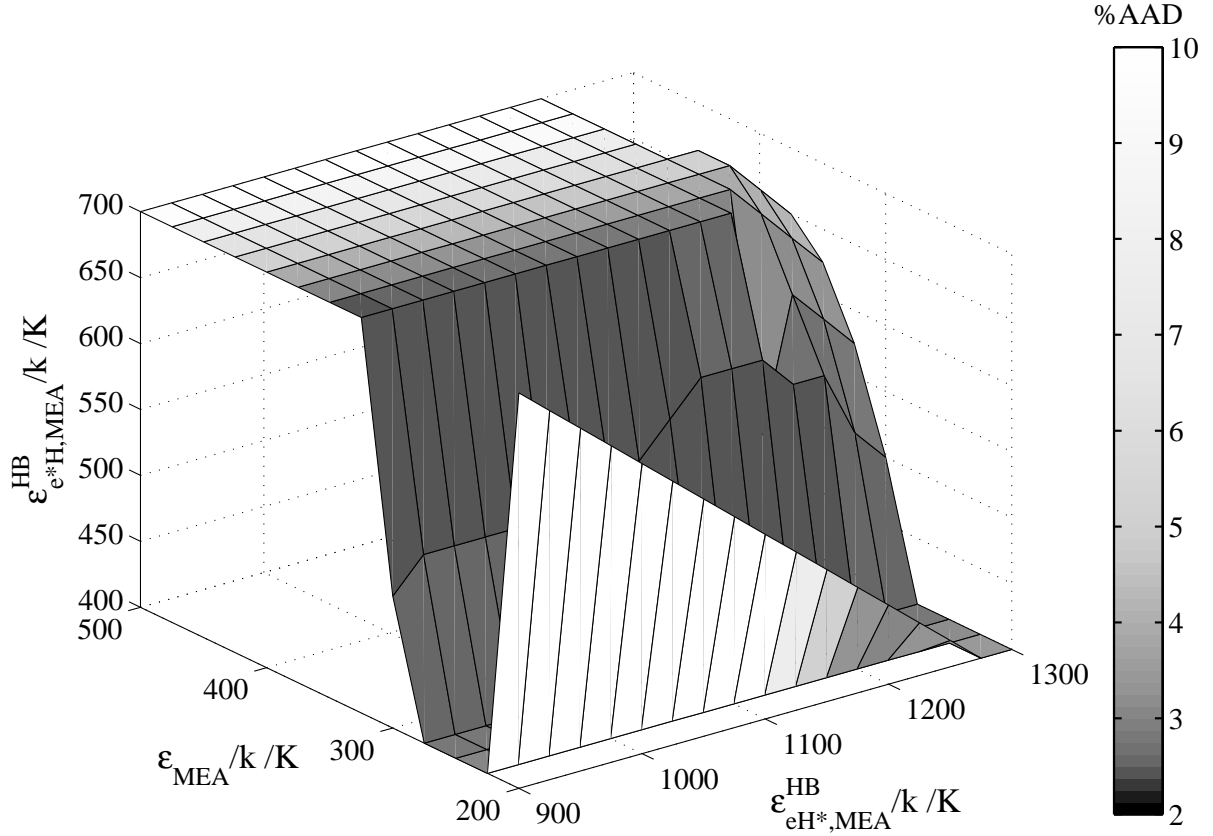


Figure 7: Contour plot for the relative average absolute deviation (%AAD) of the vapour pressure and saturated liquid density determined using the SAFT-VR equation of state with the asymmetric model of MEA. At each point on the surface, the dispersion  $\epsilon_{MEA}/k$  and self-cross-association  $\epsilon_{eH,MEA}^{HB}/k$  and  $\epsilon_{e^*H^*,MEA}^{HB}/k$  energies are fixed, and the size ( $\sigma_{MEA}$ ) and range ( $\lambda_{MEA}$ ) parameters are optimised by minimising the least-squares objective function for 376 points between the triple-point temperature to 90% of the critical point. The optimal model on this surface corresponds to %AAD  $P^{Sat} + \rho_l = 2.41\%$ . Only the relevant section of the entire parameter space explored is depicted.

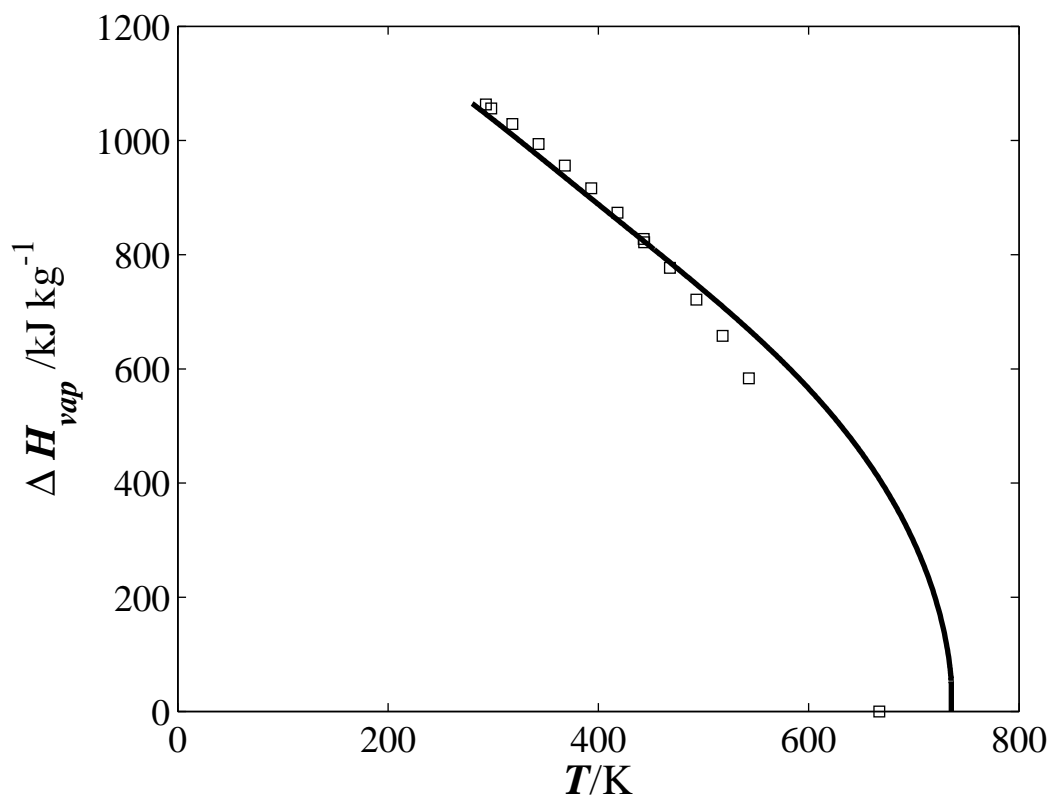


Figure 8: Experimental data (squares) [80] for the enthalpy of vaporisation  $\Delta H_{vap}$  of MEA compared with SAFT-VR predictions for the asymmetric model (continuous curve).

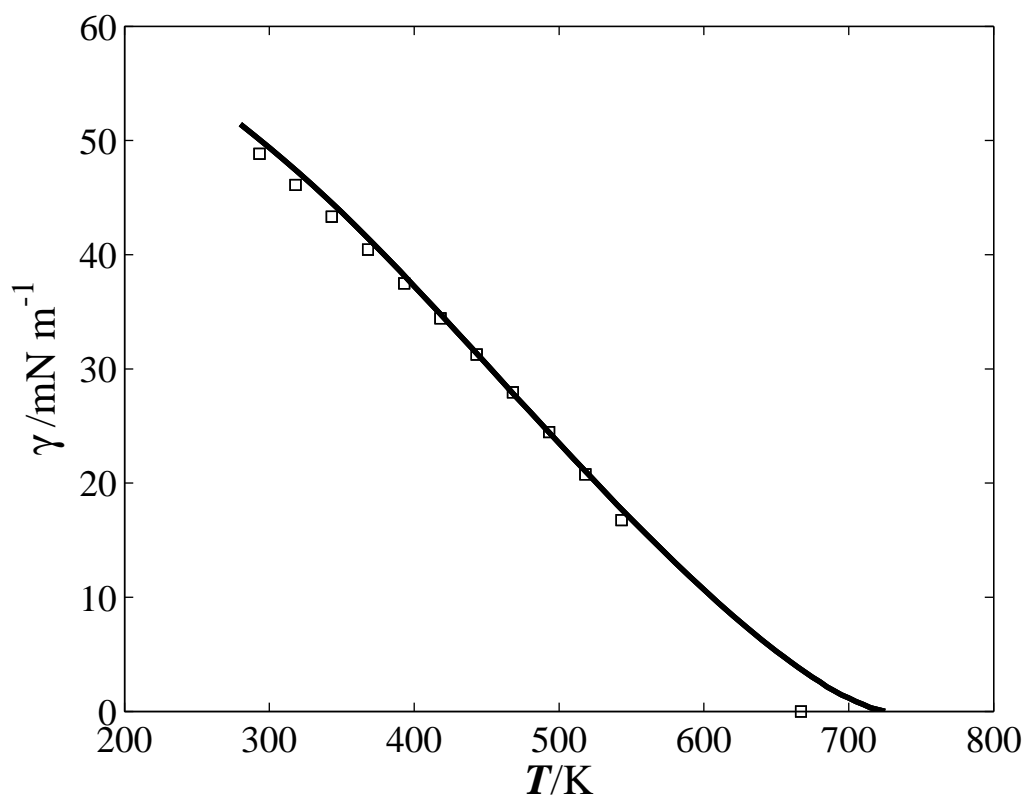


Figure 9: Experimental data (squares) [80] for vapour-liquid interfacial tension of MEA compared with SAFT-VR predictions for the asymmetric model (continuous curve).



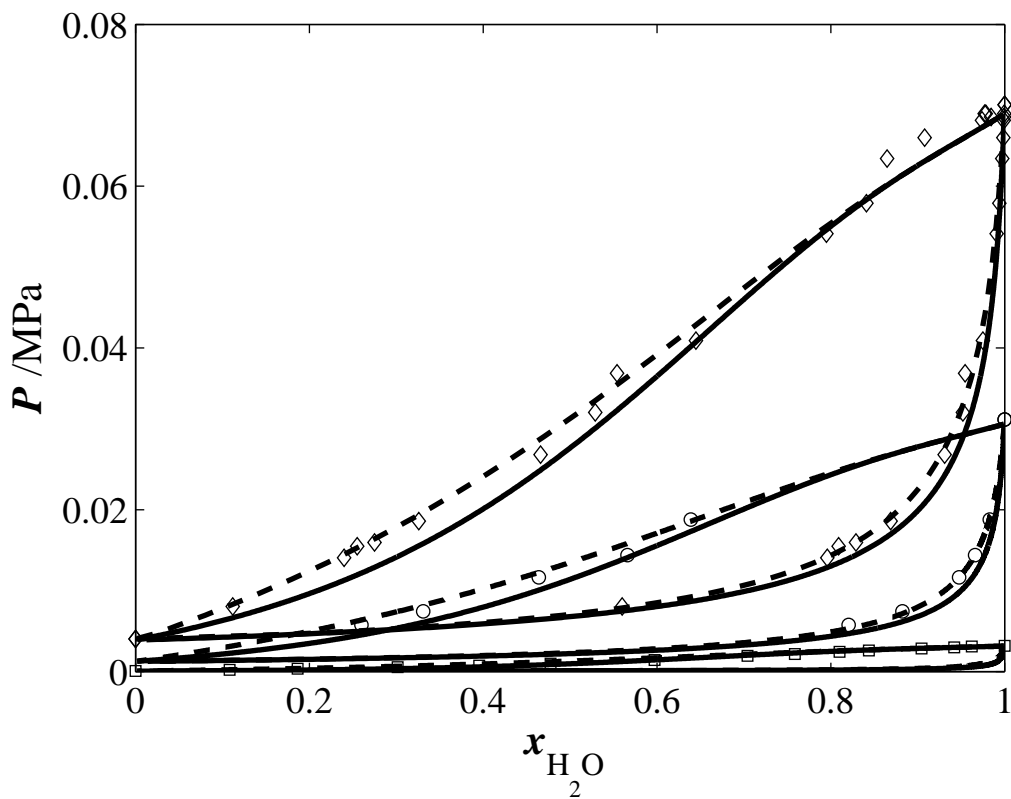


Figure 10: Isotherms of the pressure-composition ( $P-x$ ) vapour-liquid equilibria of MEA+H<sub>2</sub>O compared with SAFT-VR calculations with both the symmetric and asymmetric models of MEA. The continuous curves are the calculations with the asymmetric model of MEA and the dashed line curves those with the symmetric model of MEA. Three representative temperatures are shown:  $\square$ ,  $T = 298.15$  K;  $\circ$ ,  $T = 343.15$  K;  $\diamond$ ,  $T = 363.15$  K. The symbols correspond to the experimental data [80] and the curves to the corresponding SAFT-VR description.

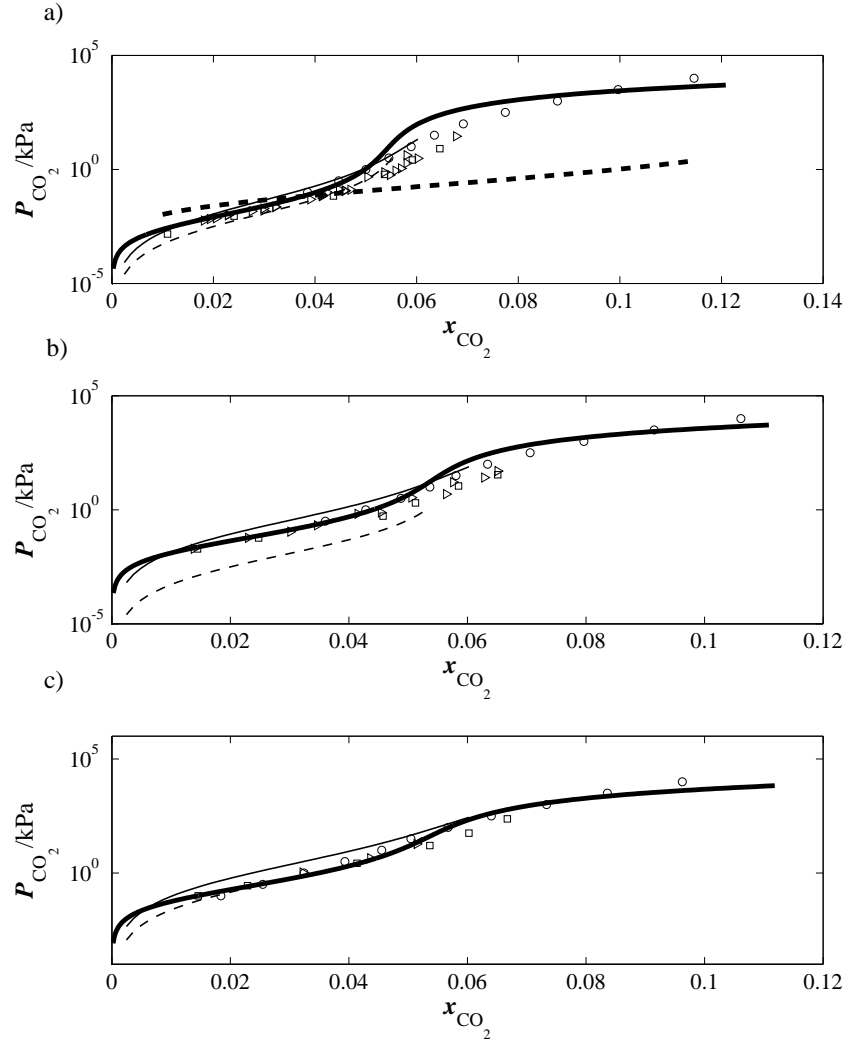


Figure 11: Isothermal projections of the pressure-composition ( $Px$ ) vapour-liquid equilibria of the ternary mixture MEA+CO<sub>2</sub>+H<sub>2</sub>O compared with SAFT-VR description: a)  $T = 313.15$  K, b)  $T = 333.15$  K, and c)  $T = 353.15$  K. The thick continuous curves correspond to SAFT-VR calculations with the asymmetric model of MEA, and the thick dashed curve in a) to SAFT-VR calculations with the symmetric model of MEA. In all figures, the thin continuous curves corresponds to a correlation presented by Aboudheir *et al.* [36] and the thin dashed curve corresponds to a correlation presented by Gabrielsen *et al.* [35] The symbols denote the experimental data:  $\square$  correspond to the data of Jou and Mather [73];  $\diamond$  and  $\triangleright$  correspond to the data of Dugas [74];  $\circ$  correspond to the data of Lee *et al.* [72]

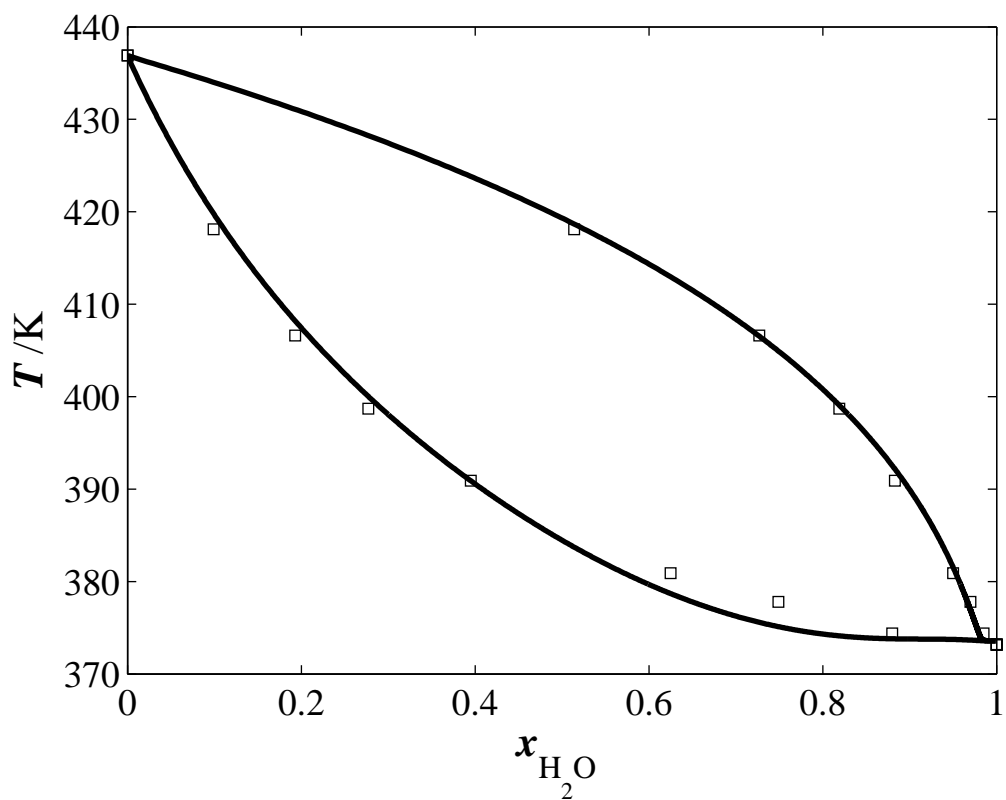


Figure 12: Binary VLE calculations for the AMP+H<sub>2</sub>O mixture compared with experimental data. The continuous lines correspond to SAFT-VR calculations and the symbols ( $\square$ ) to experimental data obtained from Pappa *et al.* [?] at a constant pressure of  $P = 0.1\text{MPa}$ .

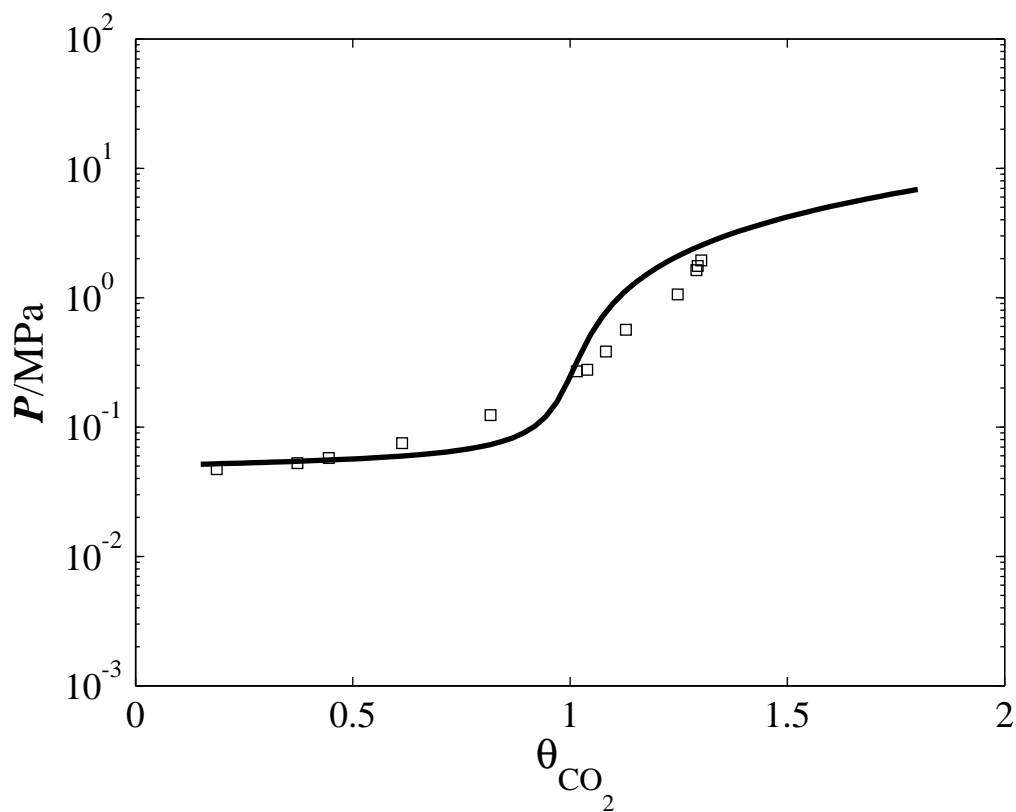


Figure 13: Ternary VLE calculations for the AMP+CO<sub>2</sub>+H<sub>2</sub>O mixture compared with experimental data. The continuous lines correspond to SAFT-VR calculations and the symbols ( $\square$ ) to the experimental data of [81] at a constant temperature of  $T = 353.15$  K

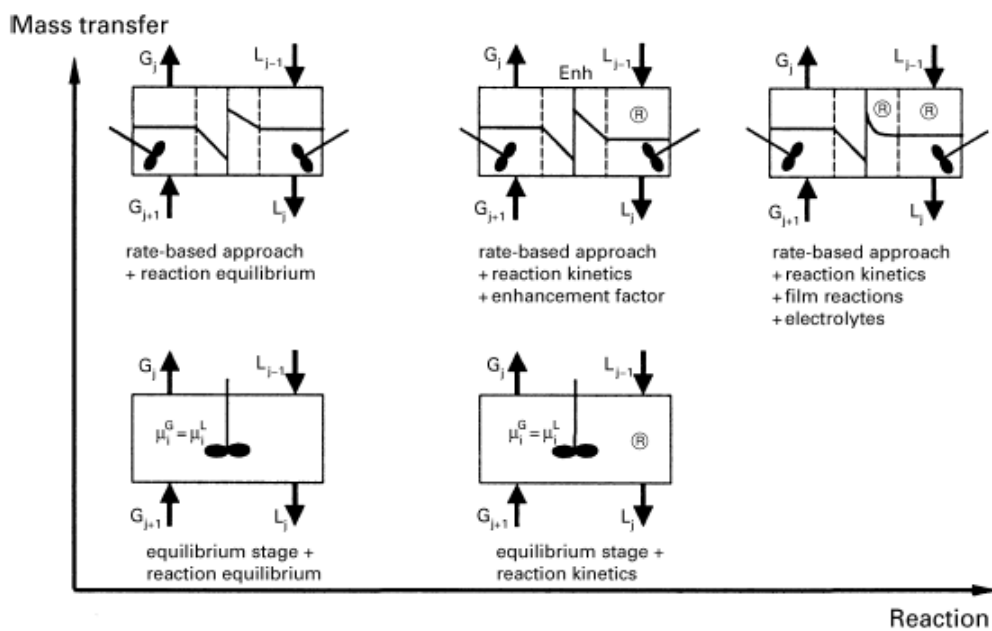


Figure 14: Evolution of model complexity, taken from Kenig *et al.* [43]

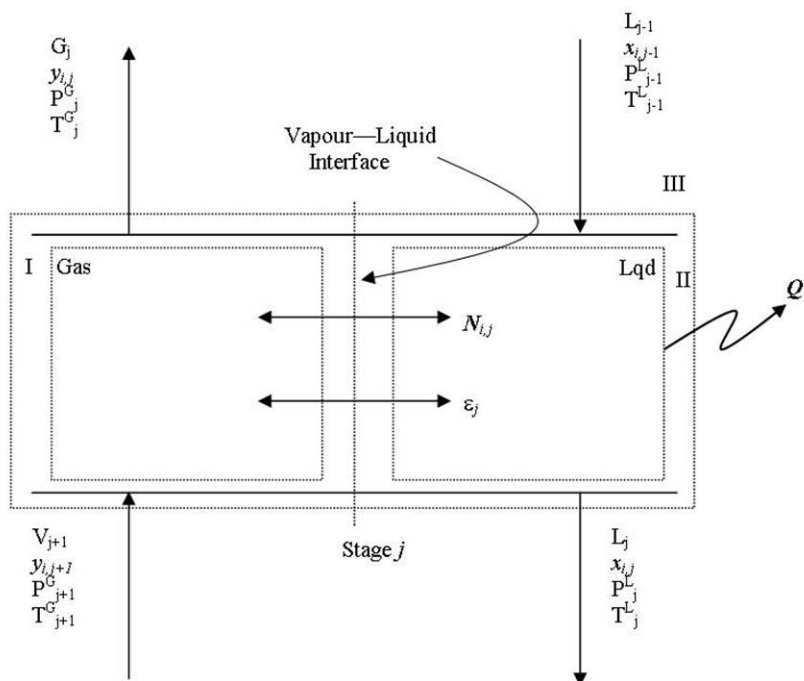


Figure 15: Representation of column stage

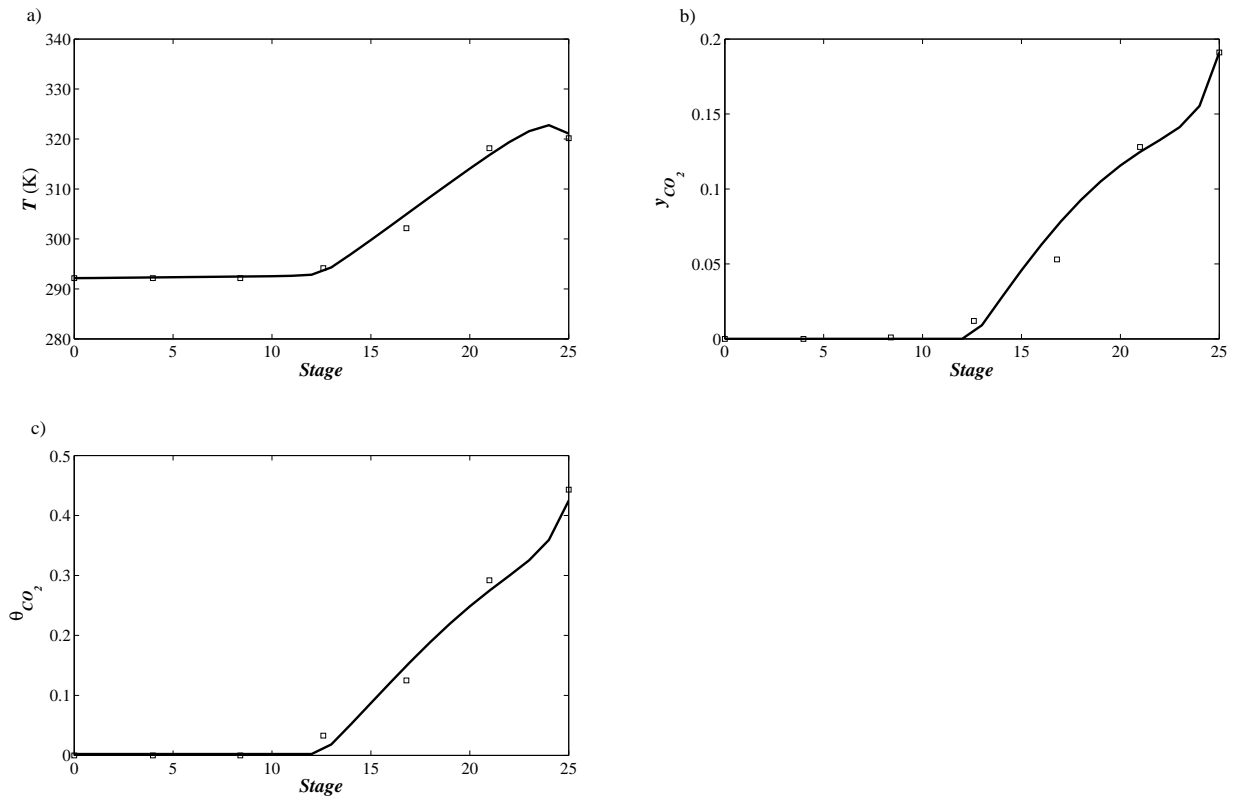


Figure 16: a) Liquid phase temperature profile for absorber column, b) Gas phase  $CO_2$  concentration profile for absorber column, c) Liquid phase  $CO_2$  loading profile for absorber column. The continuous curves correspond to the predictions of our model, and the symbols correspond to pilot plant data obtained from run T22 in [49]. Stage 1 corresponds to the top of the column, and stage 25 to the bottom. An MEA solvent is used.

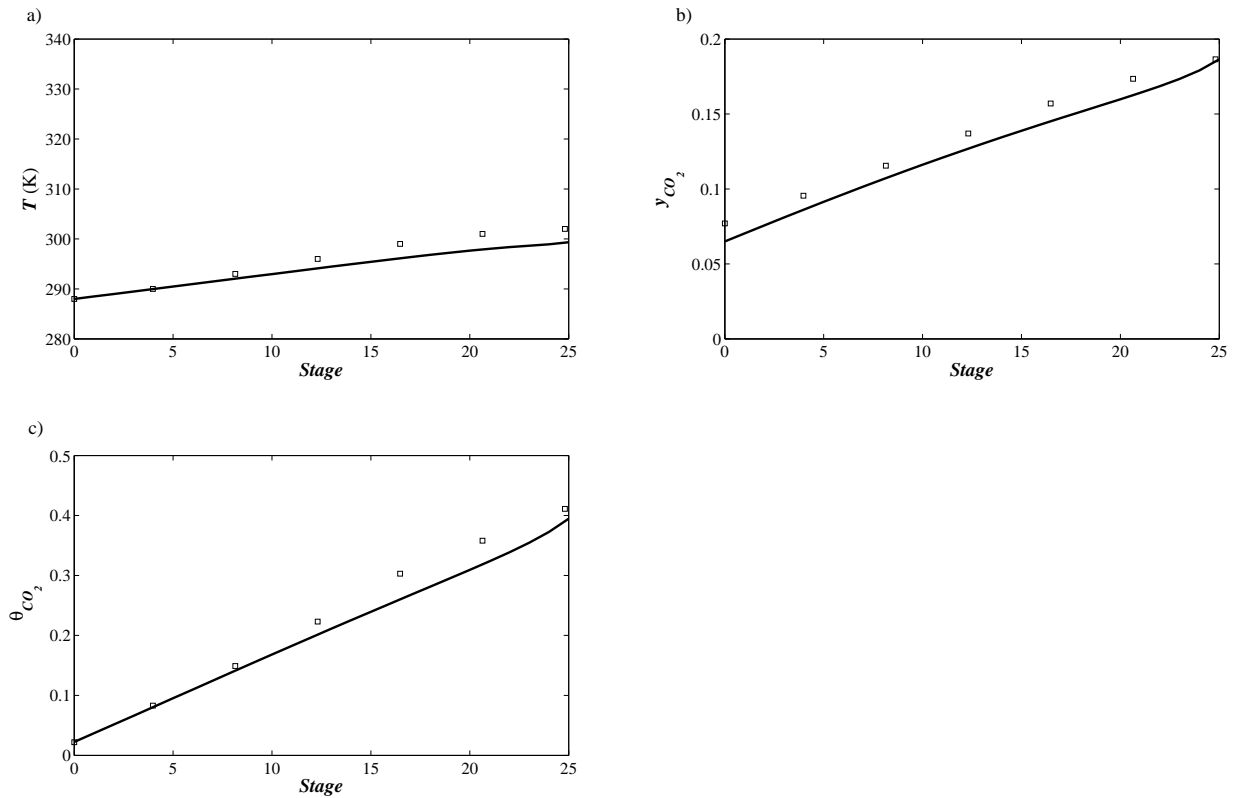


Figure 17: a) Liquid phase temperature profile for absorber column, b) Gas phase  $\text{CO}_2$  concentration profile for absorber column, c) Liquid phase  $\text{CO}_2$  loading profile for absorber column. The continuous curves correspond to the predictions of our model, and the symbols correspond to pilot plant data obtained from run T26 in [49]. Stage 1 corresponds to the top of the column, and stage 25 to the bottom. An AMP solvent is used.

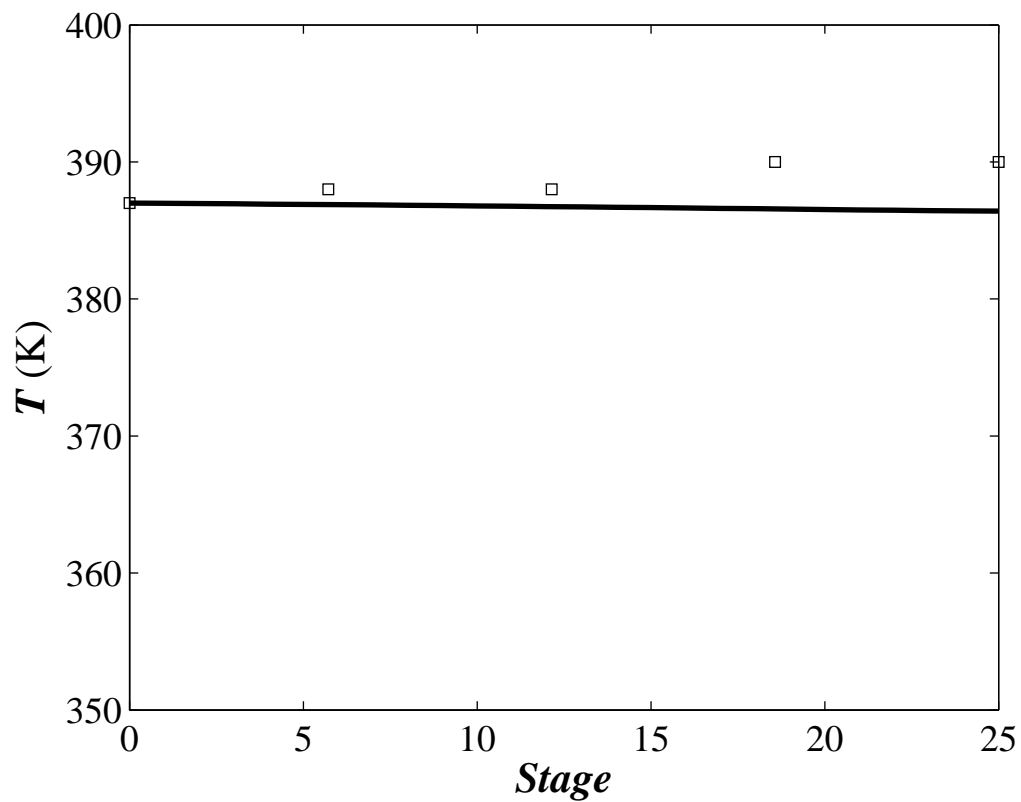


Figure 18: Liquid phase temperature profile for NTNU desorber from [77]. The continuous curves correspond to the predictions of our model, and the symbols correspond to pilot plant data. Stage 1 corresponds to the top of the column, and stage 25 to the bottom. An MEA solvent is used.



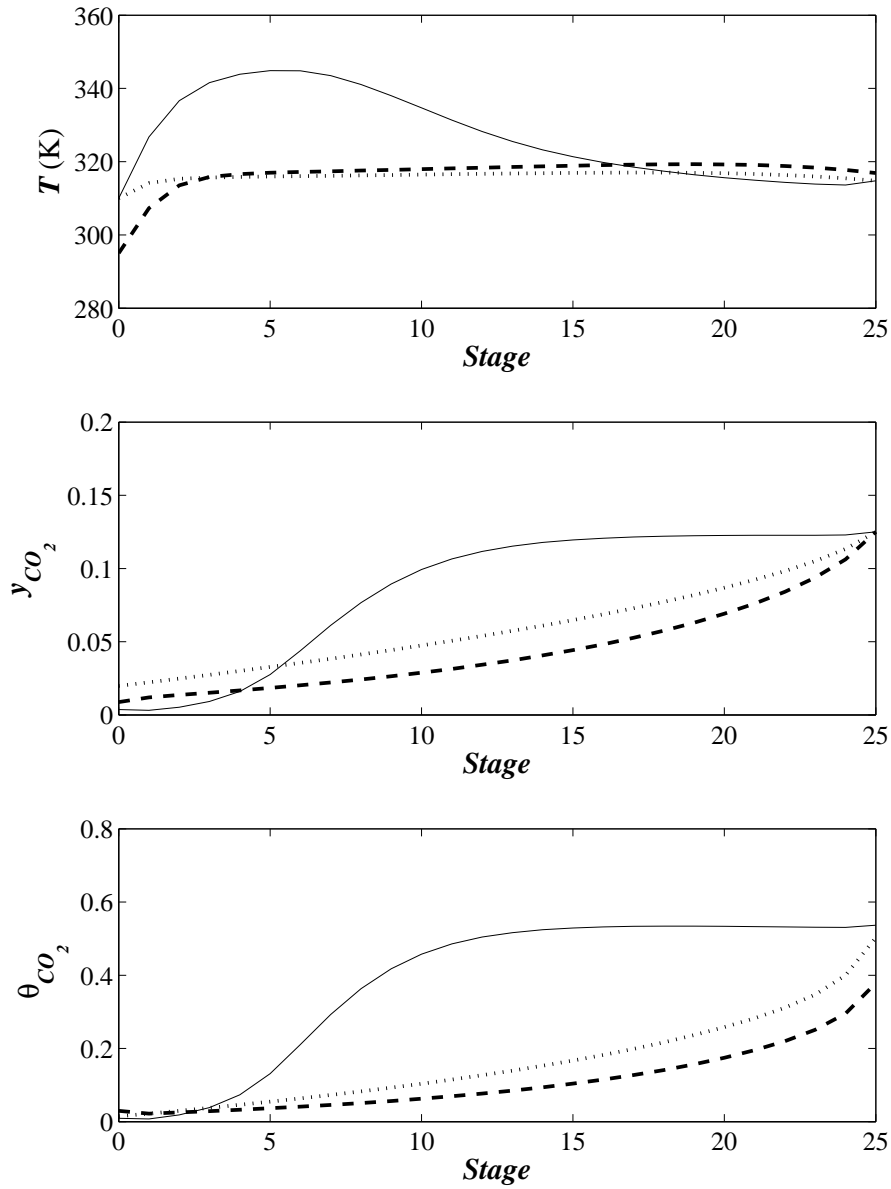


Figure 19: Predicted temperature and composition profiles for an industrial scale absorption column a) Liquid phase temperature profile b) Gas phase  $\text{CO}_2$  concentration profile c) Liquid phase  $\text{CO}_2$  loading profile. The continuous curves correspond to a 30wt% MEA solvent, the dotted curves correspond to a 30wt% AMP + 5wt%  $\text{NH}_3$  solvent blend and the dashed curves correspond to an optimised solvent blend comprising 37.7wt% AMP and 1.96wt%  $\text{NH}_3$  mixture.